Photochemistry and Spectroscopy
https://www.sciltp.com/journals/ps

Review

A La Plata Journey through Frozen Molecules: Matrix Isolation Spectroscopy Studies

Rosana M. Romano * and Carlos O. Della Védova

CEQUINOR (UNLP, CCT-CONICET La Plata, associated with CICPBA), Departamento de Química, Facultad de Ciencias Exactas, Universidad Nacional de La Plata, Boulevard 120 N 1465, La Plata 1900, Argentina
* Correspondence: romano@quimica.unlp.edu.ar

How To Cite: Romano, R.M.; Della Védova, C.O. A La Plata Journey through Frozen Molecules: Matrix Isolation Spectroscopy Studies. *Photochemistry and Spectroscopy* **2026**, *2*(1), 8. https://doi.org/10.53941/ps.2026.100008

Received: 8 December 2025
Revised: 30 December 2025
Accepted: 6 January 2026
Published: 3 March 2026

Abstract: Matrix-isolation spectroscopy is a powerful and versatile technique in physical and analytical chemistry, enabling the detailed study of highly reactive and transient species under cryogenically stabilized conditions. By trapping molecules within an inert, rigid solid matrix—typically argon, nitrogen, or krypton at temperatures as low as a few Kelvin—this method effectively quenches thermal energy, suppressing diffusion and preventing chemical decay. This review highlights the application of this foundational technique in La Plata to explore multifaceted research centred on the generation, isolation, and characterization of novel molecular entities, elucidating their fundamental properties, reaction mechanisms, and reactivity. We present examples spanning the isolation of novel compounds, detailed conformational studies, the formation and analysis of molecular complexes, and the elucidation of photochemical mechanisms. The synergy between matrix-isolation FTIR spectroscopy and computational chemistry is emphasised as a basis for validating experimental findings and advancing molecular-level understanding.

Keywords: matrix-Isolation; FTIR spectroscopy; photochemistry; novel compounds; molecular complexes; reactive intermediates; conformational equilibria

1. Introduction

Matrix-isolation spectroscopy stands as a powerful and versatile technique in physical and analytical chemistry, enabling the detailed study of highly reactive and transient species under cryogenically stabilized conditions [1,2]. A distinguished member of our La Plata Inorganic Chemistry Centre (CEQUINOR), Prof. Dr. Eduardo L. Varetti, began his foundational work in this area early in his career with a research stay in the laboratory of the pioneering chemist Georg C. Pimentel at the University of California, Berkeley, where they prepared and isolated the symmetric compound N_2O_3 in an N_2 matrix at 20 K [3].

By trapping molecules within an inert, rigid solid matrix—typically argon, nitrogen, or krypton at temperatures of a few Kelvin—this method effectively quenches thermal energy, suppressing diffusion and preventing chemical decay. The resulting cryogenic stabilization creates a unique platform for observing elusive chemical phenomena inaccessible under ambient conditions.

This review highlights research utilizing this technique to explore the generation, isolation, and characterization of novel molecular entities and the elucidation of their fundamental properties, mechanisms, and reactivity. The results and examples discussed herein correspond to investigations developed by our group over more than 30 years. A primary focus is the isolation of novel compounds, using the unique stability of the solid matrix. Specifically, we employ photolysis of molecular complexes isolated in solid matrices as a directed strategy to generate and trap unprecedented chemical structures. Selective cleavage of precursor complexes with light initiates in-situ reactions, whose unstable products are immediately stabilized by the surrounding matrix.

Complementing this approach, photochemical reactions under matrix-isolation conditions allow for the synthesis of novel species from isolated monomers, enabling stepwise spectroscopic observation of reaction pathways and definitive product identification.

Beyond preparing new molecules, a key aspect of this work is the detailed investigation of molecular conformations. The low-temperature matrix environment quenches internal rotation, allowing for the spectroscopic "freezing" of different molecular conformers. This enables the resolution and individual characterization of conformers that would rapidly interconvert in the gas phase or solution, providing crucial insights into molecular structure, stability, and intramolecular forces.

A significant portion of our investigation is dedicated to the formation and analysis of molecular complexes isolated in solid matrices, particularly those involving non-covalent interactions like hydrogen bonds and van der Waals complexes. We explore their generation via two routes: first, through the photolysis of molecular compounds isolated in solid matrices, where photofragments can recombine or interact with neighbours to form novel complexes; and second, by co-depositing different chemical species to form complexes in the gas phase, which are subsequently trapped and studied. This dual approach allows for a comparative analysis of complexation mechanisms and the critical influences of the matrix environment on intermolecular interactions.

Finally, integrating all these elements, our work elucidates photochemical mechanisms under matrix-isolation conditions. By combining controlled photoirradiation with high-resolution spectroscopic monitoring, we identify short-lived species and their interconversions. Computational chemistry critically supports the identification of these novel species by successfully reproducing experimental IR spectra, thereby validating the conclusions. Through this comprehensive methodology, we provide a deeper, mechanistic understanding of the chemical reactivity of molecular compounds studied in our group, from the initial excitation event to the formation of stable, often novel, final products.

2. Isolation of Novel Compounds in Matrix Conditions

One of the applications of the matrix isolation technique is the ability to isolate novel molecular compounds that are not stable under other conditions. This review will present two distinct strategies employed by our group. The first involves the formation of the novel species from the photolysis of a precursor compound previously isolated in the matrix. Due to the high dilutions of the precursor in the inert gas that are typical in the matrix-isolation technique, the photolysis mechanisms are predominantly unimolecular. The second strategy involves the generation of the novel species via a photochemical reaction between two species co-trapped in the same matrix site. This second pathway is favoured if the reactants form a molecular complex, as the proportion of sites occupied by both reacting species is thereby increased. As will be discussed later, in selected cases, the same species could be isolated using both mechanisms.

2.1. Isolation of Novel Species through Photolysis of Molecular Compounds Isolated in Solid Matrices

Following pioneering work isolating ClSF from FC(O)SCl [4], other molecules with the general formula XSY (X, Y = halogens) were isolated under matrix conditions (see Scheme 1). The UV photolysis of FC(O)SBr isolated in an Ar matrix—prepared earlier by the chemical reaction between FC(O)SCl and $(CH_3)_3SiBr$ at −10 °C—enabled the isolation of the previously unknown species BrSF, with the concomitant extrusion of a CO molecule [5]. This molecule was identified using FTIR spectroscopy following irradiation.

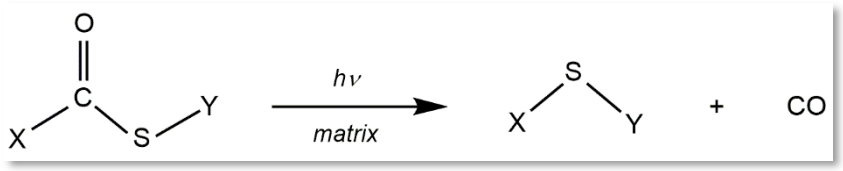

Scheme 1. Schematic representation of the isolation of XSY molecules through matrix isolation photolysis of XC(O)SY molecules, where X, Y = halogen.

Similarly, BrSCl was generated photochemically from matrix-isolated ClC(O)SBr [6]. The ClC(O)SBr was synthesized by reacting FC(O)SBr with BCl_3 and subsequently isolated in Ar, N_2, Kr, and CO-doped Ar (~5% CO) matrices at approximate ratios of 1:1000 (solute:matrix gas) to ensure unimolecular photochemical mechanisms. The matrices were then irradiated with broad-band UV-vis light and with selected spectral regions using different filters for varying time periods. An FTIR spectrum was measured after each irradiation interval.

Analysis of the spectral changes as a function of photolysis time allowed for the grouping of new IR absorptions. By considering the $^{35}Cl/^{37}Cl$ y $^{79}Br/^{81}Br$ isotopic patterns, along with computational simulations, the species BrSCl was identified as a stable entity under the experimental conditions (Figure 1). The isolation of related molecules (e.g., SCl_2 from ClC(O)SCl [7]) confirmed this general photolysis pathway involving CO extrusion (see Scheme 1). Furthermore, different species were detected during the matrix-isolation photolysis of ClC(O)SBr. A schematic representation of the general photochemical behaviour of ClC(O)SBr isolated in inert matrices at cryogenic temperatures is presented in Scheme 2. Among the products, BrC(O)SCl—a constitutional isomer of ClC(O)SBr unknown prior to this study—was detected as an intermediate. As will be discussed later, this work prompted our group to begin employing the strategy of forming novel species via in-situ matrix reactions.

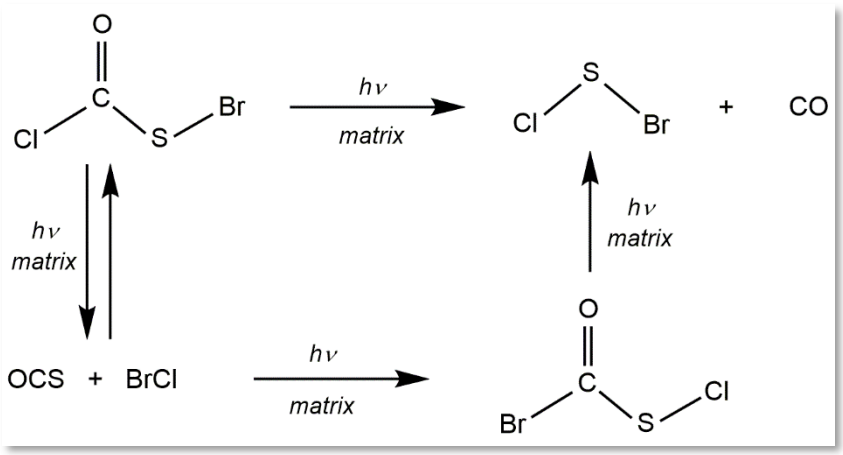

Scheme 2. Schematic representation of the mechanisms upon broad-band UV-vis photolysis of ClC(O)SBr isolated in solid matrices (for simplicity, the *syn–anti* interconversion in the pentatomic molecules was omitted).

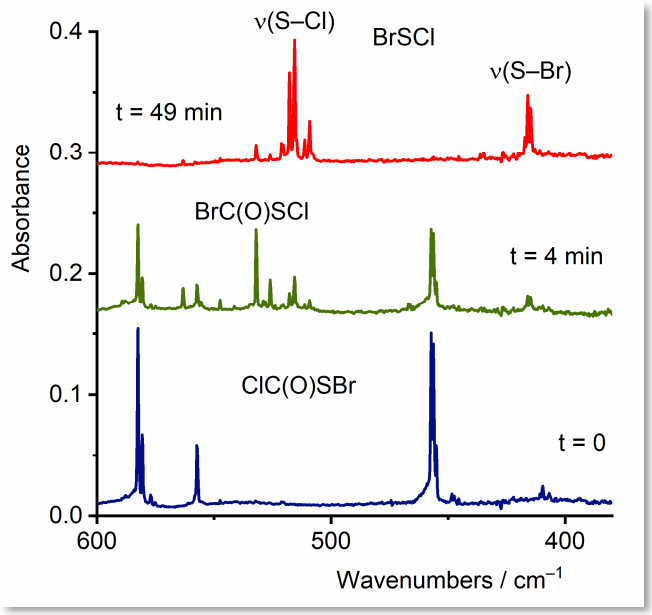

Figure 1. Selected region of the FTIR spectra of ClC(O)SBr isolated in an Ar matrix (ClC(O)SBR:Ar 1:1000) before (bottom, blue trace) and after 4 min (middle, green trace) and 49 min (top, red-trace) of broad-band UV-visible irradiation. The ν(S–Cl) absorption of the constitutional isomer BrC(O)SCl, identified by its characteristic isotopic pattern, is observed as an intermediate. The formation of the triatomic molecule BrSCl as the stable product is evidenced by the appearance of its ν(S–Cl) and ν(S–Br) bands, displaying the characteristic $^{35}Cl/^{37}Cl$ and $^{79}Br/^{81}Br$ isotopic components, respectively.

Another previously inaccessible sulfide, CH_3SF (and its perdeuterated form) was prepared by photolyzing matrix-isolated $FC(O)SCH_3$ [8]. Unlike the previous examples, CH_3SF is an intermediate. Continued irradiation induces a tautomerization, involving the detachment and migration of a hydrogen atom from the methyl group,

yielding the molecular complex $H_2C{=}S\cdots HF$ (see Scheme 3). These transformations were monitored, and the photoproducts were detected and identified by matrix IR spectroscopy. The conclusions were confirmed by studying the analogous behaviour of the perdeuterated molecule $FC(O)SCD_3$, comparing with related systems (e.g., $ClC(O)SCH_3$, CH_3SCl, and $H_2C{=}S\cdots HCl$ [7]), and by comparison with vibrational properties simulated for the different molecules by ab initio and Density Functional Theory methods. In an analogous manner, the new ethyl fluoro sulfide, $FSCH_2CH_3$, was proposed as an intermediate species in the photolysis of matrix-isolated $FC(O)SCH_2CH_3$ [9].

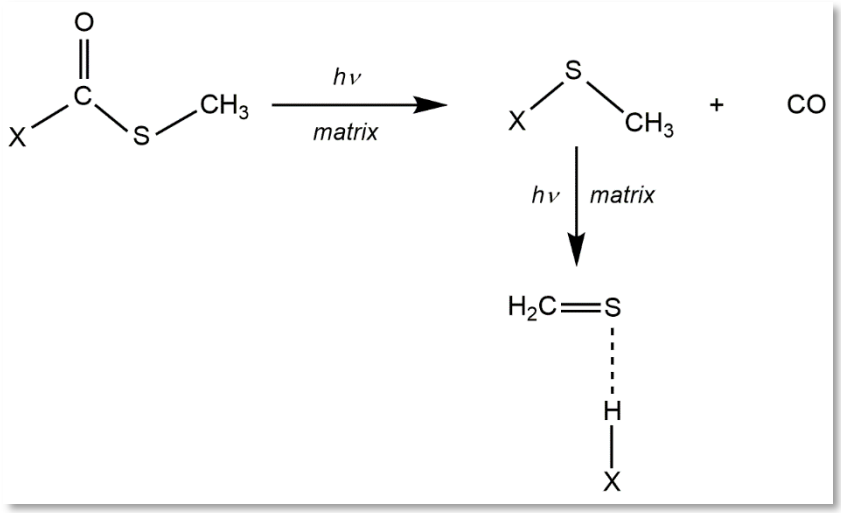

Scheme 3. Schematic representation of the matrix-isolation photolysis of $XC(O)SCH_3$ molecules where X = Cl, F.

A further example of novel species formation via this strategy is the isolation of difluoromethylselanes, XCF_2SeH (X = H, Cl), through the photolysis of the corresponding selenoacetic acids, $XCF_2C(O)SeH$ [10,11]. As in the previous cases, the mechanism is completed by the extrusion of a CO molecule. Similar to prior studies, identification relied on comparison with analogous systems where the formed species could be corroborated using literature data. Accordingly, the species CH_3SeH/CD_3SeD [12] and CF_3SeH [13] were isolated from selenoacetic acid ($CH_3C(O)SeH/CD_3C(O)SeD$) and trifluoroselenoacetic acid ($CF_3C(O)SeH$) in solid Ar, respectively.

The previously unknown molecule $CH_3CH_2OC(O)SH$ was isolated as the main photoproduct from the UV-vis photolysis of $CH_3OC(S)SC(O)OCH_2CH_3$ isolated in Ar matrix and was characterized by its matrix-isolation IR spectrum [14]. This compound was also obtained in the same work as a side-product of the reaction between potassium xanthate salts (ROC(S)SK) and ethyl chloroformate ($ClC(O)OCH_2CH_3$), and was characterized by its mass and IR spectra. Although $CH_3CH_2OC(O)SH$ had not been previously reported, its salts known and had been proposed as decomposition products during flotation processes.

2.2. Isolation of Novel Compounds through Photochemical Reactions in Matrix-Isolation Conditions

As mentioned earlier, the interpretation of the photolysis mechanisms of matrix-isolated ClC(O)SBr [6], outlined in Scheme 2, provided the conceptual foundation for producing new molecular species through a series of designed reactions under matrix conditions. The original motivation was to test the feasibility of one step in the proposed mechanism: the recombination of OCS with a halogen or interhalogen molecule to form a pentatomic molecule. To this end, these two species—which do not react in the gas phase in the absence of radiation—were mixed in a flask, diluted in a matrix gas (Ar or N_2), and subsequently deposited onto the cooled window of the matrix-isolation apparatus. The first system chosen was the reaction between OCS and Br_2, as the species BrC(O)SBr had not been obtainable by chemical methods, despite numerous attempts using different precursors, likely due to its thermodynamic instability. The mechanism was clearly corroborated by the appearance of the IR absorptions corresponding to the pentatomic species (Figure 2) [15]. This study was the first in a series of reactions that enabled the isolation of not only new species but also new families of molecules, as schematically presented in Scheme 4.

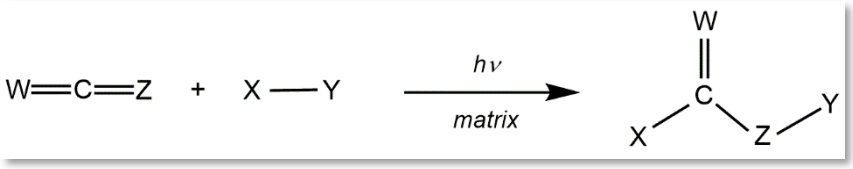

Scheme 4. Schematic representation of the matrix photochemical reaction between a triatomic molecule W=C=Z molecules (W, Z = O, S, Se) with an halogen or interhalogen molecule.

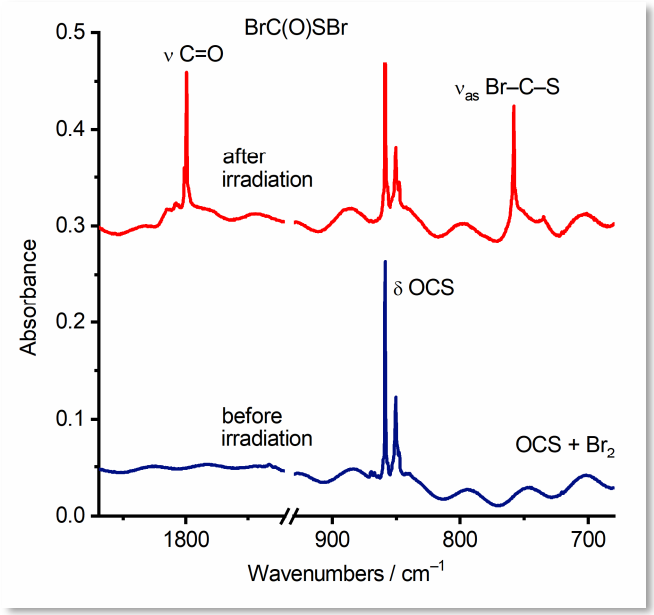

Figure 2. FTIR spectral changes in selected regions upon photolysis of a Br_2/OCS/Ar mixture (2:1:200). The bottom (blue) and top (red) traces correspond to the spectrum before and after 6 h of broad-band UV-visible irradiation, respectively. Photolysis leads to the formation of BrC(O)SBr, as evidenced by the appearance of its two most intense bands: ν(C=O) and ν_{as}(Br–C–S).

Analogously, the novel species IC(O)SBr was isolated for the first time via the photochemical reaction between OCS and IBr under matrix conditions [16]. On the other hand, several photoproducts were observed in the photochemical reactions between OCS and Cl_2 co-isolated in a matrix, with their relative yields varying with the reactant ratios. The formation of the $Cl_2C{=}O\cdots Cl_2$ van der Waals complex and ClC(O)SSCl in these experiments [16] necessarily involves a three-molecule reaction. As will be presented later, while only 1:1 adducts appear to form in mixtures of OCS and F_2, Br_2, BrF, BrCl, ICl, and IBr, 1:2 species predominate in mixtures of OCS and Cl_2 [17], explaining the differences in the photoproducts. This result highlights the role that molecular complexes formed between the reactants play in the reaction mechanisms and, consequently, in the resulting photoproducts.

Photoinduced reactions carried out in a solid Ar matrix doped with CS_2 and a dihalogen molecule XY (= Cl_2, Br_2, or BrCl) have been shown to give rise to one or more novel halothiocarbonylsulfenyl halide molecules, XC(S)SY [18]. Thus, *syn*-ClC(S)SCl, *anti*-ClC(S)SCl, *syn*-BrC(S)SBr, *anti*-BrC(S)SBr, *syn*-ClC(S)SBr, *anti*-ClC(S)SBr, *syn*-BrC(S)SCl, and *anti*-BrC(S)SCl have each been identified and characterized at least partially by their IR spectra, with findings supported by the results of quantum chemical calculations. Whereas the photochemical reactions involving CS_2 and a dihalogen molecule XY (= Cl_2, Br_2, or BrCl) led to the simultaneous formation of both the *syn* and *anti* forms of the respective halogenothiocarbonylsulfenyl halide molecule, XC(S)SY, the analogous reactions with OCS yielded only the *syn* forms of the corresponding halogenocarbonylsulfenyl halide, XC(O)SY.

Co-deposition of CS_2 and ClF in argon onto a ~15 K surface formed a $CS_2\cdots ClF$ molecular complex, identified by comparing initial matrix IR with DFT-simulated spectra [19]. While $CS_2\cdots ClF$ is calculated more stable than $CS_2\cdots FCl$, the latter's presence cannot be entirely ruled out. Broad-band UV-vis irradiation (225–800 nm) caused complete photolysis within 8 min, consistent with TD-DFT predictions. A key result is photo-induced formation and isolation of two novel pentatomic constitutional isomers: FC(S)SCl and ClC(S)SF, each identified in both *anti* and *syn* rotamers. Their formation may involve roaming F and/or Cl atoms. These molecules are

photoactive, further transforming under continued irradiation to produce CS, SCl radical, $CS_2\cdots Cl$ complex, and thiofluorophosgene (F_2CS), likely via fluorine atom migration.

Other systems explored were the photochemical reactions between carbonyl selenide (OCSe) and Cl_2 or Br_2 in solid argon at cryogenic temperatures [20]. Broad-band UV-vis irradiation yielded previously unreported ClC(O)SeCl and BrC(O)SeBr. The chlorine derivative was initially generated as the *anti* conformer and photo-isomerized to *syn* form. The brominated analogue was produced exclusively as the *syn* conformer. Identification via IR spectroscopy was validated by comparison with computed spectra.

The photochemical reaction between carbonyl selenide and chlorine monofluoride (ClF) in cryogenic argon matrices led to formation of the first interhalogen representatives of the XC(O)SeY family, obtaining both *syn* and *anti* conformers of ClC(O)SeF and FC(O)SeCl [21]. The two ClC(O)SeF conformers are generated independently, while both FC(O)SeCl isomers form via a pre-photolysis of the angular $OCSe\cdots Cl–F$ complex, preferentially yielding the less stable *anti*-FC(O)SeCl over the *syn* form. The mechanism, rationalized with quantum chemical calculations (ab initio, DFT, TD-DFT, CASSCF), involves radical processes and photoinduced electron transfer within the $OCSe\cdots Cl–F$ complex. A singlet-triplet conical intersection between *anti* and *syn* FC(O)SeCl rotamers was theoretically explored.

Reactions with molecular fluorine deserve a separate discussion. A series of photochemical reactions under matrix conditions were conducted between molecular fluorine and the triatomic molecules OCS, OCSe, CS_2, SeCS and CSe_2 [22−24]. The novel compound fluorocarbonylsulfenyl fluoride (FC(O)SF) was synthesized through photochemical reactions between OCS and F_2 in solid argon matrices, with both *syn* and *anti* conformers identified for the first time [22]. The reaction, monitored in situ by FTIR, initiates via a 1:1 $OCS\cdot F_2$ complex, primarily forming *anti*-FC(O)SF, which undergoes conformational randomization to the more stable *syn* form. Prolonged irradiation decomposes FC(O)SF via two pathways: CO extrusion yielding SF_2, and formation of difluorophosgene ($O=CF_2$). Fluorine atom migration accounts for eventual formation of SF_4 and SF_6.

UV-vis irradiation of OCSe and F_2 co-isolated in a solid argon matrix led to formation of both *syn* and *anti* conformers of FC(O)SeF [23]. The reaction proceeds via a van der Waals complex ($O=C=Se\cdots F–F$), with the *anti* conformer appearing first before randomizing to the *syn* form (see Figure 3).

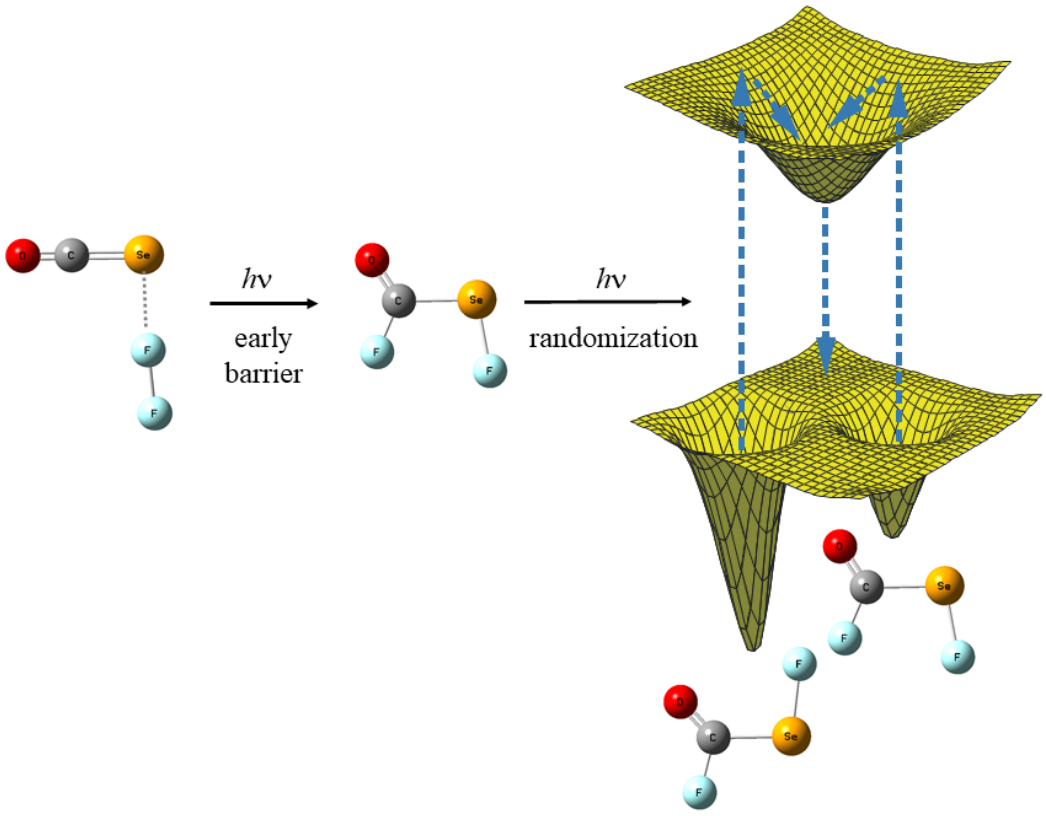

Figure 3. Schematic representation of the photochemical formation of the high-energy *anti* conformer of FC(O)SeF from van der Waals complex $O=C=Se\cdots F–F$ isolated in a solid cryogenic matrix, and a subsequent randomizing to the *syn* form.

The photochemical reactivity of F_2 with CS_2, SCSe, and CSe_2 was investigated under matrix-isolation conditions [24]. Each chalcogen-containing molecule was co-deposited with F_2 in an argon matrix, forming van der Waals complexes. Subsequent broad-band UV-vis irradiation induced reaction, synthesizing and isolating three novel pentatomic species: FC(S)SF, FC(S)SeF, and FC(Se)SeF. Each was identified as a mixture of two stable, planar conformers (*syn* and *anti*), differentiated by C=Z (Z = S, Se) orientation relative to S–F or Se–F. The relative stability depends on chalcogen atoms: the *syn* conformer is the most stable for FC(S)SF, whereas the *anti* conformer is favoured for FC(S)SeF and FC(Se)SeF. Other species from alternative pathways were also detected.

Matrix-isolation photochemistry has proven highly effective for synthesizing and characterizing carbonyl dihalides [25]. Photoinduced reactions between CO and dihalogens (Cl_2, Br_2, BrCl, ICl, IBr) in argon at ~15 K yield one or more XC(O)Y species (X, Y = Cl, Br, I). (Scheme 5) This enabled preparation and partial characterization of novel mixed carbonyl dihalides IC(O)Cl and IC(O)Br, with IR assignments corroborated by calculations. These phosgene-type molecules are stable and efficiently formed after two hours of irradiation. The mechanism is initiated by photodissociation of the dihalogen. Subsequent halogen atom addition to CO is modulated by matrix cage effects and product photolability. Evidence for halogen atom intermediacy includes detection of the angular ClCO· radical. Notably, the formation of $O=CBr_2$ in the photochemical reaction between CO and Br_2 proceeded with a very low yield. This difference from the analogous reactions was explained by the absence of BrCO·, radical formation, which has not been detected to date. Instead, a Br···CO, complex, detected for the first time in this study, is formed. To enhance yield of compounds like BrC(O)Cl, IC(O)Cl, IC(O)Br, $OCCI_2$, (see Scheme 5) a promising strategy is external generation of halogen atoms followed by co-deposition with CO, potentially providing evidence for ICO· radical.

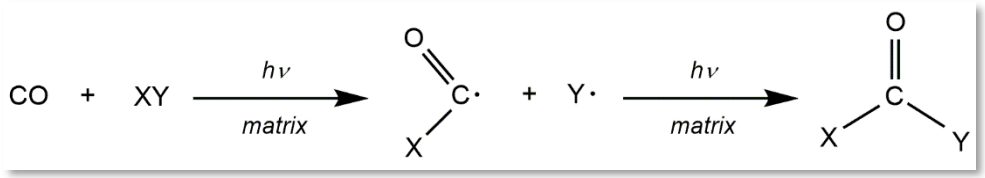

Scheme 5. Proposed photochemical reaction mechanism for the matrix-isolated reaction between carbon monoxide and a halogen or interhalogen molecule (X = F, Cl, I and Y = F, Cl, Br, I).

In summary, reactions between two reactants under matrix conditions, assisted by light, have proven to be a highly suitable strategy for the isolation of novel species from the XC(W)ZY and XC(O)Y families, where X, Y = F, Cl, Br, I and W, Z = O, S, Se. These studies demonstrate the importance of pre-formed molecular complexes deposited in a single matrix site prior to photolysis in directing the reaction, as well as the involvement of reactive intermediates such as free radicals in the formation of the products.

3. Conformational Studies

Matrix-isolation IR spectroscopy is a remarkably powerful technique for conformational analysis. Trapping molecules in a rigid, inert solid at cryogenic temperatures eliminates broad, overlapping bands originating from vibro-rotational structure (in the gas phase) and intermolecular interactions (in condensed phases). This yields sharp spectral features that resolve absorptions from individual conformers with very similar energies. Furthermore, selective irradiation can induce conformational interconversion (rotamerization), providing direct experimental evidence for assigning spectral features.

3.1. Conformational Randomization via Photoinduced Interconversion

The pentatomic species XC(W)ZY (X, Y = halogen and W, Z = chalcogen) discussed in the previous section present a conformational equilibrium between two planar structures: a *syn* form (where the C=W double bond is *syn* with respect to the Z–Y single bound) and an *anti* form (where the C=W double bond is *anti* with respect to the Z–Y single bound), as illustrated in Figure 4.

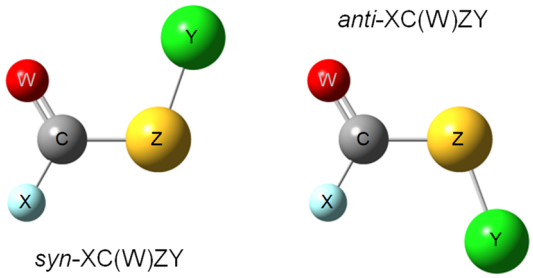

Figure 4. Molecular models of the *syn*- and *anti*-conformer of XC(W)ZY molecules.

Photoinduced interconversion between these rotamers has been observed, leading to conformational randomization—a stationary state where the population of each form is approximately 50%. This phenomenon can be explained by a transition to an excited state whose energy minimum geometry coincides with the maximum on the ground state potential energy surface, causing the molecule to decay with equal probability into each of the ground state minima. This process is schematically depicted in Figure 3.

Examples include species with the general formula FC(O)SY (where Y = Cl, Br), for which an equilibrium between the *syn* and *anti* forms has been detected. A method to experimentally determine the conformational composition of a molecule is Gas Electron Diffraction (GED), a technique that obtains information about molecular geometry by analysing the scattering of an electron beam through a vaporized sample. For FC(O)SCl, GED determined a free-energy difference of 1.2(3) kcal·mol^{-1} (uncertainty refers to 3σ), while the value calculated from matrix IR spectra was 1.4(1) kcal·mol^{-1} (based on relative band intensities; uncertainty corresponds to 3σ). Irradiating N_2 or Ar matrices with UV light (λ < 300 nm and broad-band, respectively) caused a drastic change in the IR spectrum due to photolytic interconversion, particularly evident in the carbonylic stretching region (Figure 5) [26]. This behaviour was corroborated by Raman spectroscopy before and after irradiating an Ar-matrix containing FC(O)SCl, which allowed observation of other relevant spectral regions [27].

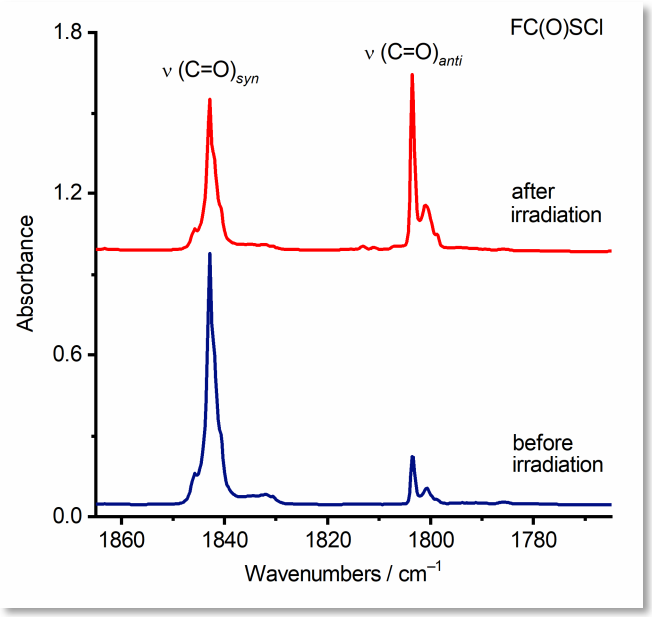

Figure 5. FTIR spectra in the ν(C=O) region of FC(O)SCl isolated in an Ar matrix (FC(O)SCl:Ar 1:1000) before (bottom, blue trace) and after (top, red trace) 6 min of broad-band UV-visible photolysis. The photolysis drives a conformational randomization process, as evidenced by the intensity changes of their respective ν(C=O) bands.

The advantages of observing the randomization process are twofold. First, it allows for the clear distinction of IR and Raman signals belonging to each conformer, serving as a valuable tool for correct spectral assignment. Second, it enables the estimation of relative absorptivity coefficients (IR) or polarizability factors (Raman), assuming a stationary state with approximately 50% of each conformer is reached. A second example is the study of the conformational equilibrium of FC(O)SBr. Similarly, a randomization process was observed after irradiating

the matrix, allowing for the estimation of a room-temperature vapour composition of approximately 91% *syn* and 9% *anti* forms [5].

The situation is different for derivatives where X = Cl, such as ClC(O)SCl and ClC(O)SBr. Initially, only the *syn* conformer is detectable in the FTIR spectra of these matrix-isolated compounds. However, due to the high sensitivity of matrix spectra and interconversion after UV irradiation, it was possible to detect the higher-energy *anti* form. For ClC(O)SCl, matrix-isolation spectroscopy revealed that the *anti* conformer constitutes less than 1% of the vapour molecules at ambient temperature [7,28]. These findings were consistent with quantum chemical calculations and low-temperature X-ray crystallography, which confirmed the exclusive presence of the *syn* rotamer (C_s symmetry) in the solid state. Similarly, the initial FTIR spectrum of matrix-isolated ClC(O)SBr showed the vapour to consist of more than 99% of the *syn* form in equilibrium with less than 1% of the *anti* conformer [6]. After irradiation caused conformational randomization, it led to a roughly equimolar mixture of the two rotamers. In both cases, the approximately 100 cm^{-1} difference between the carbonylic stretching wavenumber between the *syn* and *anti* forms aligns well with computational predictions.

Light-induced conformational interconversion has also been observed in other species. For example, $XC(O)SCH_3$ (X = F, Cl) and $FC(O)SCH_2CH_3$ exhibited similar behaviour. The photolytic interconversion of the two rotamers $FC(O)SCH_3/FC(O)SCD_3$ was the first process observed upon broad-band UV-vis irradiation of the matrix-isolated molecule [8]. The unambiguous identification of IR absorptions due to the less stable *anti* rotamer allowed the conclusion that the vapour is composed of approximately 98% of the *syn* form and 2% of the *anti* form at ambient temperatures, in good agreement with quantum chemical calculations forecasts.

The conformational landscapes of $ClC(O)SCH_3/ClC(O)SCD_3$ were elucidated, with key evidence from matrix-isolation IR spectroscopy [7]. High-resolution IR spectra in cryogenic matrices confirmed overwhelming predominance of the *syn* rotamer in the vapour phase, with a contribution of the *anti* form < 1%.

S-ethyl fluorothioformate ($FC(O)SCH_2CH_3$) was investigated using vapour-phase IR, liquid Raman, and IR in Ar/N_2 matrices at ~12 K [9]. At room temperature, a rich conformational equilibrium exists, dominated by the most stable form of C_1 symmetry where the C=O bond is *syn* to S–C(sp^3) bond and the C–C bond is *gauche* to the C–S bond. A second conformer of C_s symmetry (*syn-anti*) was also identified. From nozzle temperature variation data, the ΔH between the C_1 and C_s forms was determined to be 0.45 kcal mol^{-1}. A third species (*anti-gauche*) was detected only after UV-vis irradiation, which successfully induced conformational interconversion.

Conformational interconversion was also observed for matrix-isolated methoxycarbonylsulfenyl chloride, $CH_3OC(O)SCl$ [29]. A multi-technique approach showed a clear preference for the *syn* form, exclusive in the low-temperature crystalline solid. This stability, validated by NBO analysis, is attributed to significant anomeric effects.

The conformational landscape of trifluoroacetyl triflate, $CF_3C(O)OSO_2CF_3$, was elucidated through Ar matrix-isolation FTIR spectroscopy before and after broad-band UV-vis irradiation [30]. High-resolution spectra confirmed the presence of two conformers in the vapour deposited at room temperature. The light-induced conformational randomization aided the assignment of the IR absorptions and allowed for a quantitative analysis, which determined that the vapour at room temperature consists of approximately 60–70% of the *syn-anti* conformer and 30–40% of the *syn-gauche* form.

This strategy once again demonstrated its potential in the study of 1,1,3-trichlorotrifluoroacetone, $Cl_2FCC(O)CClF_2$, a perhalogenated acetone of atmospheric interest [31]. Stable conformers were identified through a combination of theoretical (2D PES, DFT, MP2 optimization) and experimental methods (FTIR of gas at different temperatures, Ar/N_2 matrices with varying ratios, FT-Raman of liquid). The interpretation of the complex spectra was guided by theoretical calculations. Definitive conformational proof was obtained from broad-band UV-vis irradiation of the matrices, which promoted rotamerization and allowed for the monitoring of corresponding IR spectral changes. Furthermore, UV-vis absorption profiles at different pressures were compared with TD-DFT calculations for the individual rotamers.

A comprehensive investigation into constitutional and rotational isomerism of FC(O)SCN and FC(O)NCS provided highly relevant matrix-isolation data [32]. Both isomers exist as an equilibrium of two conformers (C_s symmetry) in gaseous and liquid states, distinguished by *syn* or *anti* C=O orientation relative to SCN/NCS. For FC(O)SCN, the enthalpy difference ΔH = H(*anti*) − H(*syn*) was determined to be 0.9 ± 0.2 kcal·mol^{-1} from a van't Hoff plot analysis of matrix-isolation IR data (experimental uncertainty). Kinetics of thermal *anti* to *syn* conversion for FC(O)NCS was investigated in Ar/N_2 matrices; reverse *syn* to *anti* photoisomerization was induced with UV-vis light. A constitutional rearrangement was observed upon irradiation: FC(O)SCN converts to FC(O)NCS in neat liquid/solution; conversely, 193 nm irradiation of matrix-isolated FC(O)NCS caused rearrangement to FC(O)SCN (Scheme 6).

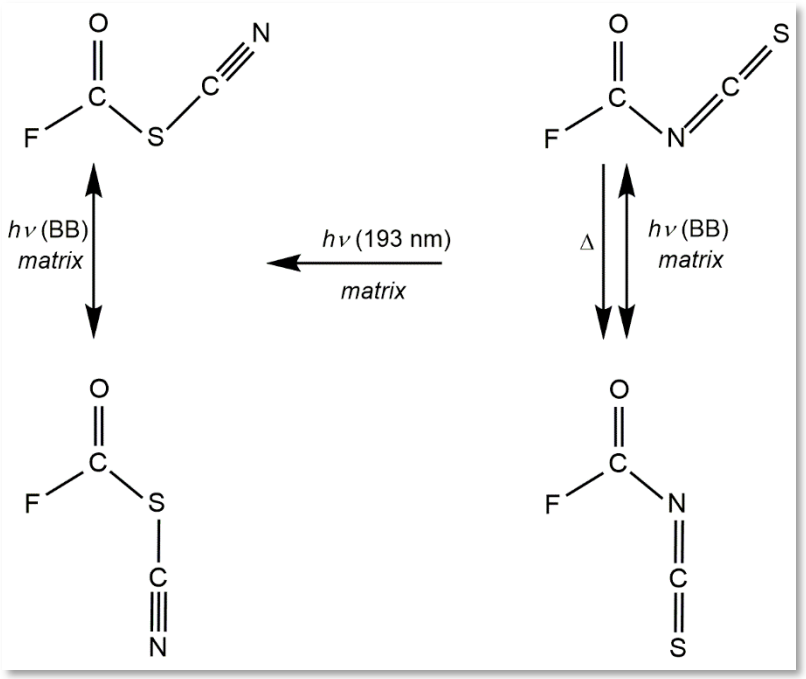

Scheme 6. Schematic representation of the proposed photochemical isomerization pathways for FC(O)SCN and FC(O)NCS isolated in solid matrices.

Constitutional isomers chlorocarbonylthio- and isothiocyanate (ClC(O)SCN and ClC(O)NCS) were comprehensively characterized [33]. Matrix-isolation revealed coexistence of *syn* and *anti* conformers in the gas phase. For ClC(O)SCN, the *syn* conformer is more stable, with an enthalpy difference $\Delta H°$(*anti/syn*) = 1.3(0.3) kcal·mol^{-1} determined from a van't Hoff plot (experimental uncertainty). In contrast, for ClC(O)NCS, the *anti* conformer is more stable—a finding supported by GED. Furthermore, matrix isolation enabled the determination of an unusually low *syn* to *anti* interconversion barrier of 0.98(0.15) kcal·mol^{-1} at cryogenic temperatures, derived from an Arrhenius plot (experimental uncertainty). Matrix-isolation photolysis showed ClC(O)SCN converts to ClC(O)NCS under UV-vis irradiation.

Vapours of acetyl isothiocyanate ($CH_3C(O)NCS$) and trifluoroacetyl isothiocyanate ($CF_3C(O)NCS$) were isolated in solid argon at 15 K [34]. Matrix-isolation FTIR confirmed rotational isomerism in both, demonstrated by temperature-dependent IR spectra and changes induced by broad-band UV-vis irradiation (200–800 nm). Initial spectra revealed two conformers each. Matrix-isolation enabled study of distinct photochemical pathways: $CH_3C(O)NCS$ undergoes conformational randomization while decomposing; $CF_3C(O)NCS$ primarily decarbonylates.

The photolysis of FC(O)SSCl—a compound prepared for the first time by our group—was investigated in solid argon [35,36]. The primary photoprocess was the conformational *syn–gauche* → *anti–gauche* isomerization, followed by a rich photochemistry, which will be discussed later. A similar photochemical behaviour was observed for the chlorinated analog, ClC(O)SSCl [37].

3.2. Conformer-Specific Formation from Precursors

The situation is different for cases, described previously, where the species is generated by photolysis of a precursor (e.g., BrC(O)SCl [6]), or by reactions between triatomic species W=C=Z and halogens or interhalogens XY [15,16,18−24]. In these experiments, the preferential formation of one conformer over the other depends more on the geometry of the pre-reactive molecular complex than on the relative stabilities of the conformers. Therefore, the relative band intensities in the spectra cannot be directly related to the free energy differences between them, although light-induced interconversion still allowed for the characterization of the spectral signals for each conformer. A detailed description of the results for each case was provided in the previous section.

Findings from these numerous cases are unified by the common XC(W)ZY structural backbone, motivating a systematic comparative investigation [38]. A computational study of 72 XC(W)ZY molecules (B3LYP/aug-cc-pVDZ) determined *syn/anti* energy differences, revealing clear dependence on the identity of the halogen (X, Y) and chalcogen (W, Z). For the XC(O)SY and XC(O)SeY species, the *syn* conformation is consistently the most stable. The energy difference favoring *syn* form increases with the atomic number of X and Y (F < Cl < Br). The relative stability of the *anti* form in XC(O)SeY is nearly identical to that in XC(O)SY. For XC(S)SY and XC(S)SeY

molecules, the *anti* rotamer is preferred for X = F, Cl, while for Br, the energy differences are small, with a slight preference for the *syn* form. In contrast, the *anti* rotamer is invariably predicted as the most stable for XC(Se)SeY compounds (see Figure 6).

Furthermore, the relative stabilities of constitutional isomers were compared. For all halogen combinations: XC(O)SY > XC(S)OY; XC(O)SeY > XC(Se)OY; XC(S)SeY > XC(Se)SY. For isomers resulting from halogen exchange, the structure with the lighter halogen bonded directly to carbon is always favoured. Computational predictions show a strong linear correlation with available experimental data. Conformational preferences are primarily governed by a balance of electronic interactions. While anomeric effects stabilize *syn* rotamer, the decisive factor is conjugative interaction, which dictates the prevalent conformation. Although electrostatic, steric, and dipole-dipole interactions may play a role, a model focusing on conjugative and anomeric effects serves to explain the observed behaviour, highlighting their fundamental importance.

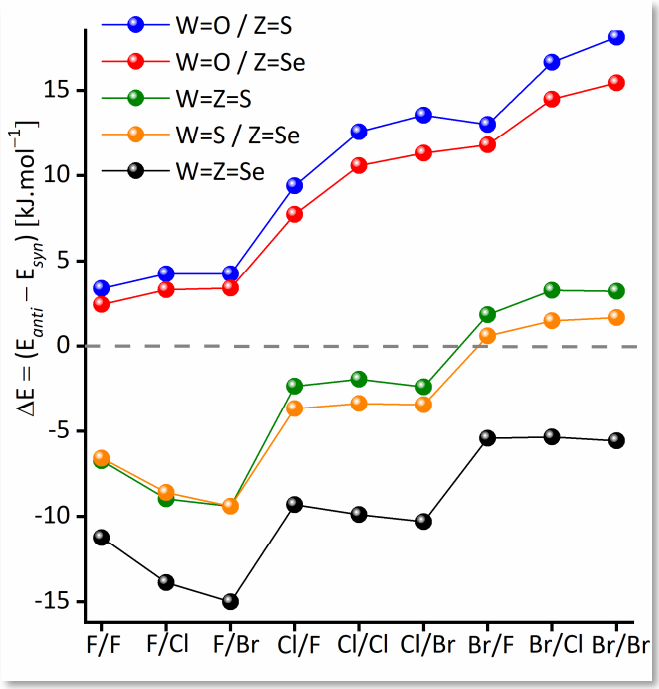

Figure 6. Energy differences with zero-point corrections (in kJ·mol^{-1}) between the *anti*- and *syn*-forms of XC(W)ZY molecules, with W/Z = O, S, Se and X/Y = F, Cl, Br, calculated with the B3LYP/aug-pVDZ approximation (from Ref. [38]).

3.3. Elucidation of Complex Conformational Landscapes

Matrix-isolation IR spectroscopy is equally powerful for characterizing conformational equilibria in systems where the initial distribution is determined by thermal energy, providing a high-resolution snapshot of the gas-phase composition. For instance, a multi-technique study fluorocarbonyl trifluoromethanesulfonate, $FC(O)OSO_2CF_3$, combined gas electron diffraction (GED), vibrational spectroscopy, and X-ray crystallography [39]. Matrix-isolation IR quantified the gas-phase equilibrium, revealing a mixture dominated by the *trans* conformer (59 ± 5%), with the *gauche* conformer as the minor component (based on relative band intensities; experimental uncertainties). This result is consistent with GED data, which yielded a composition of 67 ± 8% *trans* (3σ uncertainty). In a comparative analysis, the chloro analogue, $ClC(O)OSO_2CF_3$, also showed the equilibrium dominated by the *trans* form (66 ± 8%) in the gas-phase, though low-temperature X-ray crystallography surprisingly revealed the coexistence of both *trans* and *gauche* forms in the crystal lattice, stabilized by specific packing forces [40,41].

The technique is particularly valuable for resolving complex multi-conformer systems. As demonstrated for bis(chlorocarbonyl)trisulfane, ClC(O)SSSC(O)Cl, matrix-isolation IR analysis revealed the coexistence of three conformational forms, in excellent agreement with quantum chemical predictions [42]. Similarly, for (methoxycarbonyl)(2-propoxythiocarbonyl) sulfide, $(CH_3)_2CHOC(S)SC(O)OCH_3$, the liquid-phase IR spectrum suggested a simple equilibrium, but matrix-isolation unveiled a more complex situation involving three distinct conformers, whose structures were elucidated theoretically [43]. This ability to "freeze out" and resolve individual conformers was further demonstrated in novel selenocarboxylic acids, such as $CH_3C(O)SeH$ [12] and $CF_3C(O)SeH$ [13]

where two conformers were identified, and in, $HCF_2C(O)SeH$ and $ClCF_2C(O)SeH$, which exhibited equilibria involving two and three conformers, respectively [10].

Matrix-isolation often provides superior resolution compared to other spectroscopic methods. This advantage is clear in the case of perfluoropropanoyl fluoride, $CF_3CF_2C(O)F$, gas-phase FTIR failed to clearly evidence the minor *anti* conformer, but its presence was unequivocally confirmed by matrix-isolation FTIR, highlighting the technique's sensitivity [44]. Likewise, this approach was also key in determining the conformational composition of $CF_2BrC(O)F$, where the simplified spectra provided direct experimental proof of the overwhelming dominance of the *gauche* conformer [45]. For compounds like trichloromethyl chloroformate ($ClC(O)OCCl_3$), matrix-isolation data conclusively demonstrated the existence of a single conformational form, corroborated by a significant calculated energy difference to the hypothetical *anti* rotamer [46].

The power of matrix-isolation extends to intricate structural problems, such as the complex conformational behaviour of perfluoropropionic acid, $CF_3CF_2C(O)OH$, where it helped identify three distinct monomeric conformations and a dimeric structure [47]. Comprehensive analyses of other molecules, such as thioacetic acid [48], xanthogen ethyl formates [14], diallyl sulfide [49], chlorodifluoroacetyl cyanide [50], ethyl chloroformate [51], have consistently relied on matrix-isolation to experimentally validate computationally predicted conformational distributions.

Another illustrative case is disulfuryl dichloride, $ClSO_2OSO_2Cl$, studied by two different, independent methods [52]. While the refinement of the gas-phase diffraction data utilized only one conformer, in the temperature dependent matrix-isolated vibrational spectra three different conformers could be identified (Figure 7). A related example involves the *syn*−*gauche* and *syn*−*anti* conformers of $ClC(O)OSO_2Cl$. Both conformers were detected in the Ar-matrix FTIR spectrum. However, gas-phase electron diffraction (GED) analysis confirms only the presence of the *syn*−*gauche* rotamer, while the existence of the *syn*−*anti* conformer can be neither confirmed nor excluded by the GED experiment [53].

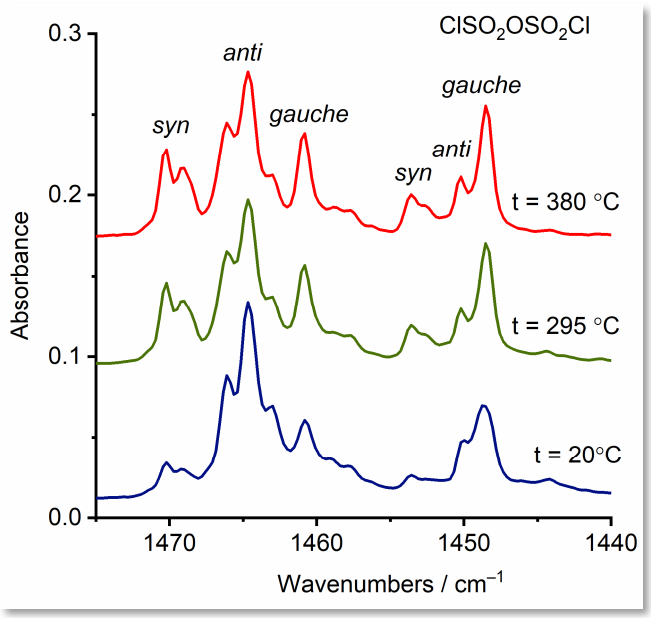

Figure 7. Conformational composition of gaseous $ClSO_2OSO_2Cl$ as a function of temperature. FTIR spectra (selected regions) were recorded after isolation of the gas in an Ar matrix (1:1000). from a nozzle held at 20 °C (bottom, blue-trace), 295 °C (middle, green-trace), and 380 °C (top, red-trace). The spectra reveal the presence of three conformers (*anti*, *gauche*, and *syn*), whose relative populations are temperature-dependent.

The conformational equilibria of chlorodifluoroacetyl isocyanate, $ClF_2CC(O)NCO$, and chlorodifluoroacetyl isothiocyanate, $ClF_2CC(O)NCS$, were elucidated using a combined approach of matrix-isolation IR spectroscopy, gas electron diffraction (GED), and quantum chemical calculations [54,55]. Both molecules were confirmed to exist as two conformers in the gas phase, each featuring a *gauche*-oriented C–Cl bond relative to the C=O group, but differing in the *syn* or *anti* orientation of the C=O group relative to the N=C bond of the NCO/NCS group. For $ClF_2CC(O)NCO$, the experimental enthalpy difference between the more stable *syn-gauche* and the *anti-gauche* form was determined to be $\Delta H° = 1.3 \pm 0.2$ kcal mol^{-1} from a van't Hoff plot analysis of FTIR matrix data (experimental uncertainty) This value aligns reasonably with the computed value of 0.8 kcal mol^{-1} obtained at the B3LYP/6-311+G(3df) level of theory [54]. For $ClF_2CC(O)NCS$, the corresponding free energy difference was

$\Delta G° = 0.63$ kcal mol^{-1}, as calculated at the B3LYP/6-31G(d) level [55]. For both compounds, the key structural parameters of the dominant *gauche–syn* conformer were precisely determined by GED.

The technique proved crucial in a multi-technique investigation elucidated the molecular structure and conformational equilibrium of $(CH_3)_3CSNO$, marking the first experimental determination of geometrical parameters for an S-nitrosothiol species in the gas phase [56]. Electron diffraction revealed the coexistence of *anti* and *syn* conformers, with the *syn* form less abundant. Vibrational spectroscopy, with matrix-isolation IR playing a pivotal role, determined an *anti:syn* population ratio of ~80:20 at room temperature, in excellent agreement with MP2(full)/cc-pVTZ predictions. This equilibrium is also present in the liquid phase, as evidenced by UV/Vis and resonance Raman spectra.

Further demonstrating its versatility, matrix-isolation was applied to 1,1-dicyano-2-chloro-2,2-difluoroethyl chlorodifluoroacetate, $CClF_2C(O)OC(CN)_2CClF_2$, and the analogue $CF_3C(O)OC(CN)_2CF_3$ using combined experimental and computational approaches [57]. Matrix-isolation IR spectroscopy coupled with quantum chemical calculations revealed distinct behaviours. For $CClF_2C(O)OC(CN)_2CClF_2$, computational models predicted four rotamers; Ar-matrix IR confirmed two conformers—*gauche-syn-gauche* and *gauche-syn-anti*—with the former predominating at ambient temperature. In contrast, $CF_3C(O)OC(CN)_2CF_3$ exhibited a single conformational structure (*syn-syn-anti*).

As a final example showcasing the depth of information obtainable, the conformational landscape of the novel diacetyl diselenide, $CH_3C(O)SeSeC(O)CH_3$, was unravelled. This compound was synthesized for the first time via oxidation of selenoacetic acid ($CH_3C(O)SeH$). Matrix-IR spectra provided direct evidence of a conformational equilibrium in the gas phase at room temperature, interpreted by considering two of three stable rotamers identified from a 3D potential energy surface scan. NBO analysis revealed that the conformational stability order is governed by vicinal hyperconjugative interactions involving lone pairs on Se or O atoms delocalizing into σ* orbitals of C=O, C–C, and Se–C bonds [58].

4. Molecular Complexes Isolated in Solid Matrices

Cryogenic matrix isolation spectroscopy is an ideal technique for studying interacting species, ranging from weak molecular complexes to structures with stronger interactions, such as adducts. Our research group has employed two distinct methods to isolate such complexes. The first method involves the photolysis of an isolated species within the matrix. In this approach, following photolysis and the eventual fragmentation of a molecule, the resulting fragments remain trapped in the same matrix cage. This constrained environment is highly conducive to interaction and complex formation.

The second method involves the co-deposition of the two precursor species using our group's standard pulsed deposition technique. In this setup, the molecular complex under study can originate either from a pre-formed association in the gas phase before deposition, or its formation can be directly promoted by the pulsed deposition process itself, which enhances interactions between the species as they condense onto the cold surface.

In certain cases, we have successfully formed the same complex using both methods. A comparison reveals a key distinction: while the photolysis method can yield species with varying relative stabilities, the co-deposition method typically isolates only the thermodynamically most favorable structures. Furthermore, irradiation of these pre-formed systems can also lead to the formation and identification of higher-energy forms.

4.1. Molecular Complexes Formed through Photolysis of Molecular Compounds

The photolysis of $XC(O)SCH_3$ (X = F, Cl) isolated in solid matrices led to the generation of CH_2=S···H−X loose complexes, mediated by the formation of the CH_3SX species with the concomitant extrusion of a CO (Figure 8) [7,8]. The formation of the complexes was clearly evidenced by drastic changes in the H−X stretching wavenumbers, with shifts of −435 cm^{-1} for HF and −364 cm^{-1} for HCl in Ar-matrices, along with small changes in the signals from the CH_2=S moiety. This finding was correctly predicted by computational methods and explained by NBO analysis, which indicated stabilization of the complex arises from the interaction of the lone pair on the S atom of CH_2=S with the unfilled σ* antibonding orbital of the HX molecule.

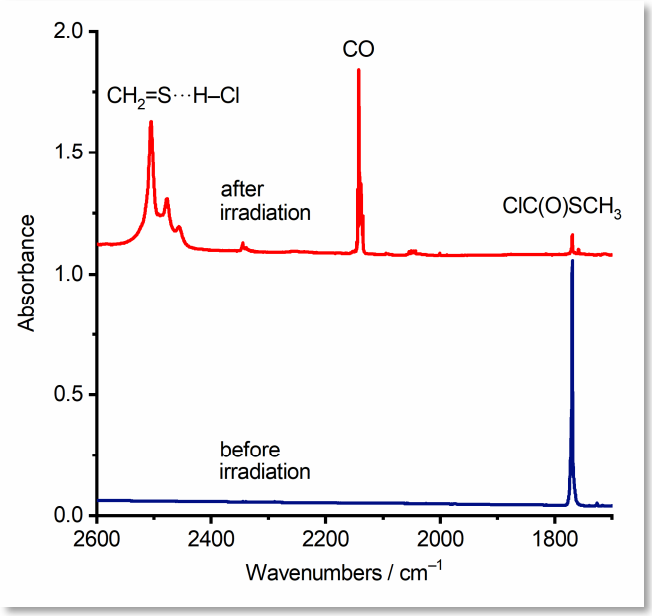

Figure 8. Selected region of the FTIR spectra of $ClC(O)SCH_3$ isolated in an Ar matrix (1:1000) before (bottom, blue-trace) and after 100 min of broad-band UV-visible photolysis (top, red-trace). The photolysis leads to the formation of CO and a CH_2=S···H–X complex, identified by the appearance of its characteristic ν(H–Cl) absorption band.

Molecular complexes between ketene (CH_2=C=O) and H_2S, CH_3SH, and $CH_3C(O)SH$, were formed from the UV-vis photolysis of $CH_3C(O)SR$ molecules (R = H, CH_3, and $C(O)CH_3$, respectively) isolated in solid matrices [48]. The photochemical channel leading to these species, schematized in Figure 9, contrasts with the fragmentation routes of XC(O)SY molecules where X, Y = halogen (see Scheme 2). The difference between these processes and the one leading to ketene formation originates from the photolability of the acetyl group, where detachment of a hydrogen atom from the methyl group is the dominant mechanism.

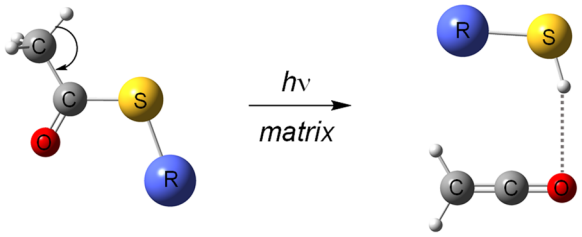

Figure 9. Formation of CH_2=C=O···HSR molecular complexes following UV-vis photolysis of $CH_3C(O)SR$ precursors (R = H, CH_3, $C(O)CH_3$).

As previously mentioned, the photolysis of XC(O)SY molecules (X, Y = halogen) is dominated by two distinct mechanisms ([6,7], and references cited therein). One leading to OCS and XY photoproducts, and the other to XSY and CO (see Scheme 2). As the two subunits are confined within the same matrix cage, the formation of the respective molecular complex occurs. These examples will be discussed in the next subsection, together with the description of the same molecular complexes formed by mixing the two components in gas-phase.

The photochemical behaviour of $ClSO_2NCO$ and FSO_2NCO isolated in solid argon is a remarkable example [59]. After broad-band UV-vis irradiation, products were characterized by IR spectroscopy. The compounds exhibited different photostabilities. $ClSO_2NCO$ experienced a two-step decomposition: primary photolysis generated a 1:1 SO_2:ClNCO complex; subsequent irradiation decomposed ClNCO via parallel channels (forming ClNO, NO, CO, ClCO·), while SO_2 (transitioning from complexed to uncomplexed) remained photostable. The structure of the SO_2:ClNCO complex was explored using ab initio/DFT methods; theory supports a model where an SO_2 oxygen lone pair interacts with the σ*(Cl–N) orbital of ClNCO. In contrast, FSO_2NCO was highly photostable; only trace amounts of FNCO and CO were detected.

Several molecular complexes were identified during the photolysis of FC(O)SSCl: CO···ClSSF, OCS···ClSF, OCS···ClF, CO···ClSF, CS_2···ClF. Their identification was performed by comparing experimental

IR spectra with DFT simulations, except for OCS···ClF, which was assigned based on reported IR absorptions [35]. In addition to these species, the molecules FC(O)SCl and ClFC=O (accompanied by the loss of one or two S atoms) were also formed as a consequence of the photofragmentation.

4.2. Molecular Complexes Formed in Gas-Phase and Studied by Matrix-Isolation Spectroscopy

Structural and vibrational characteristics of weakly bound 1:1 CO···XY complexes (XY = Cl_2, BrCl, ICl, IBr) were elucidated using matrix-isolation IR spectroscopy by depositing gas mixtures of the two molecules with the inert gas, aided by DFT calculations [60]. Two families of linear complexes exist, differentiated by whether the C or O terminal of CO interacts with the dihalogen. For heteronuclear XY, binding can occur at either the X or Y atom, leading to four potential isomers. The blue shift in the ν(CO) mode characterizing complexes of the type OC···XY can be interpreted in terms of the slight antibonding character of the lone pair orbital localized mainly on the carbon atom of CO. The magnitude of Δν(CO) increased in the order: OC···Cl_2 < OC···Br_2 < OC···BrI ≤ OC···ClI < OC···BrCl < OC···IBr < OC···ICl. When CO coordinates through its oxygen atom, the ν(CO) mode undergoes a red shift, reflecting the bonding character of the oxygen lone pair. The ν(XY) mode of some of the OC···XY complexes was detected as red-shifted relative to the monomers, including for the OC···Cl_2 species, for which the ν(Cl_2) mode was identified with its characteristic isotopic pattern.

Molecular complexes of OCS with F_2, ClF, Cl_2, BrCl, Br_2, or ICl were isolated in solid matrices [17,23]. The IR spectra were interpreted as arising from 1:1 complexes, although trimer species were predominant in mixtures of OCS and Cl_2. Alternatively, 1:1 adducts between OCS and ClF, Cl_2, or BrCl were generated through broad-band UV-vis photolysis of matrix-isolated FC(O)SCl, ClC(O)SCl, or BrC(O)SCl, respectively. These two alternative pathways for complex formation are schematically illustrated in Figure 10.

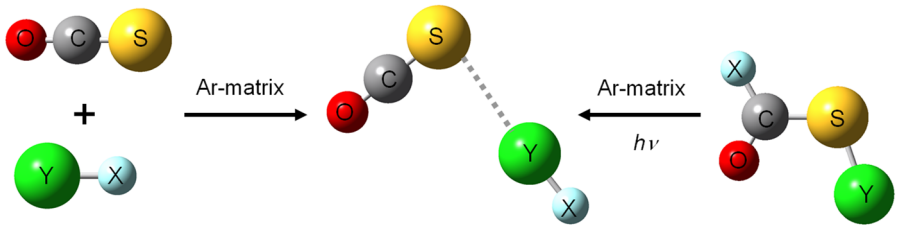

Figure 10. Schematic representation of the two alternative formation pathways for molecular complexes of OCS with dihalogens and interhalogens: Co-deposition and matrix isolation (left), in-situ generation via broad-band UV-visible photolysis of the corresponding XC(O)SY compounds (right).

Mixtures of CS_2 and dihalogens/interhalogens yielded 1:1 van der Waals complexes [19,24,61]. For every CS_2/XY system, calculations confirm the complex is more stable than isolated constituents. For heteronuclear XY, computations predict two isomeric structures (X or Y interacting with CS_2), both with positive binding energy. Mirroring the CO-dihalogen complexes, the structure coordinated through the less electronegative halogen is consistently more stable. The formation of the respective complexes with CS_2 can be observed through the activation of the Cl–Cl and Br–Br stretching modes. These complexes have been proved to act as pre-reactive species necessary for the photochemical formation of XC(S)SY molecules [18,19,24].

A 1:1 CS_2···HCl complex was generated in the gas phase and isolated in an argon matrix for FTIR characterization (Figure 11) [62]. The ν(HCl) vibrational mode exhibited a significantly larger red-shift upon complexation with CS_2 than with CO_2 or OCS, indicating a strong hydrogen-bonding interaction. This trend mirrors that observed for HF complexes with CS_2, CO_2, and OCS. The principal contribution to the energy stabilisation of the CS_2···HCl complex originates from the interaction between a non-bonding orbital on the sulphur atom (the donor) and the vacant antibonding σ* orbital of the HCl molecule (the acceptor). This orbital interaction, schematised in Figure 12, accounts for the intermolecular angles (∠CS···H) being close to 90°.

A CO_2/N_2 heteroaggregate with a T-like structure was detected during the study of carbon dioxide isolated in an Ar-matrix [63]. The sensitivity of the technique is so high that this complex was detected even with N_2 present only as an impurity, a finding later corroborated by doping the matrix with increasing amounts of N_2.

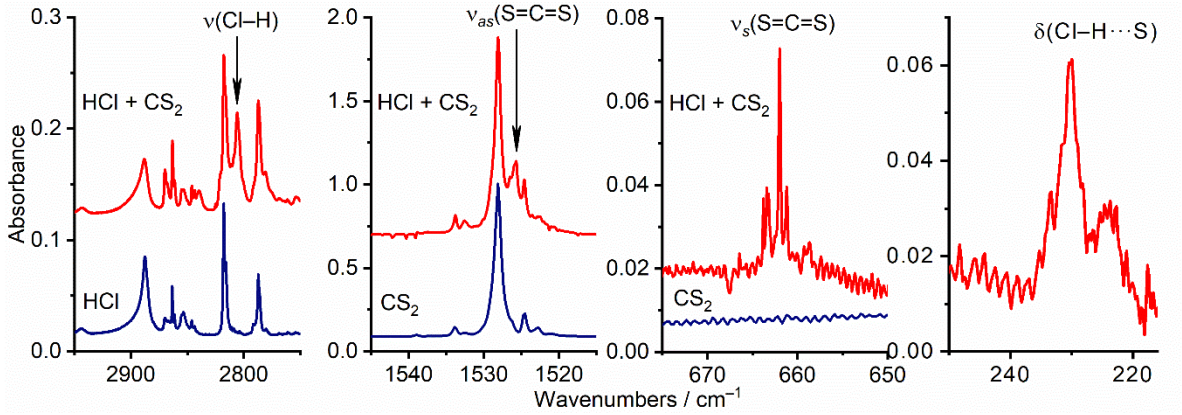

Figure 11. FTIR spectra in selected regions of an HCl:CS_2:Ar (2:1:200) matrix (red-traces) are compared to the spectra of the isolated components, HCl:Ar (1:100) and CS_2:Ar (1:200) (blue-traces). Absorptions assigned to the CS_2···HCl complex are indicated.

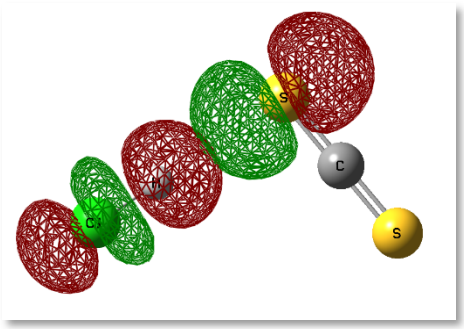

Figure 12. Schematic representation of the $n_S \rightarrow \sigma^*$ (H-Cl) orbital interaction in the CS_2···HCl complex, based on Natural Bond Orbital (NBO) analysis.

Interaction between bromomethane (CH_3Br) and water was investigated to understand heteroaggregate formation by co-depositing CH_3Br and H_2O at varying concentrations in argon [64]. From the FTIR spectra before and after annealing, a 1:1 CH_3Br:H_2O complex, formed even with minimal proportion of water, and a 1:2 CH_3Br:$(H_2O)_2$ heteroaggregate were identified. Comparative studies with CH_3Cl showed similar behaviour, forming analogous CH_3Cl:H_2O heteroaggregates. This demonstrates a general halomethane affinity for water, suggesting atmospheric reactivity could be modified via such interactions—a factor relevant for atmospheric models.

In a recent study, mixtures of phosphorus pentafluoride (PF_5) and acetonitrile (CH_3CN) were isolated in solid Ar to investigate the possible formation of either a complex or an adduct [65]. This work was motivated by the goal of gaining a deeper understanding of the synthesis process of $LiPF_6$, a dominant lithium-ion battery electrolyte salt, which involve the reaction of PF_5 dissolved in CH_3CN with LiF. While two possible structures for the 1:1 species are predicted as stable, only the global minimum was identified in the matrix IR spectra. This identification was corroborated by the behaviour of the bands after annealing. The model that best aligning with the experimental data involves a dative interaction where the nitrogen lone pair of CH_3CN binds to the phosphorus atom of PF_5, forming an adduct and producing a drastic change in the symmetry of the PF_5, clearly reflected in the IR spectrum. This provides molecular-level insight into the initial interactions fundamental to understanding $LiPF_6$ formation.

4.3. Studies of Molecular Homoaggregates

Varying the ratio between a target species and the matrix gas is a highly useful method for detecting homoaggregates, as the signals corresponding to these species are expected to increase in relative intensity as their concentration in the mixture increases. Annealing the matrix also allows for clear identification of these species. The presence of bands attributable to homoaggregates, and their relative intensities compared to isolated monomers, is indicative of their stability. With the aid of comparison with theoretical models, it is possible, particularly for simple species, to correlate the observed spectrum with the aggregate's structure.

Following this approach, our group, in a reinvestigation of the CO_2 dimer, proposed a parallel-displaced structure for $(CO_2)_2$, represented in Figure 13, based on an analysis of the dimer's IR spectrum, which is composed of fundamental bands—including the activated symmetric stretching mode—and non-fundamental modes [63].

Dimeric and trimeric structures of CS_2 were also identified through a combined experimental (FTIR in Ar and N_2 matrices) and theoretical approach [66]. Similarly, various dimeric forms of OCSe isolated in solid Ar/N_2 were detected (Figure 14) [67]. While broad-band UV-vis irradiation of the OCSe monomer led to its decomposition into a perturbed CO molecule by the Se atom, the dimeric form decomposed primarily to $(CO)_2$.

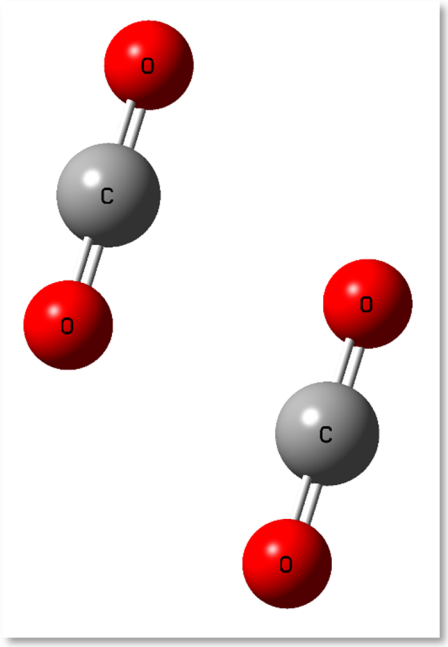

Figure 13. Molecular model of the parallel-displaced structure for carbon dioxide dimer.

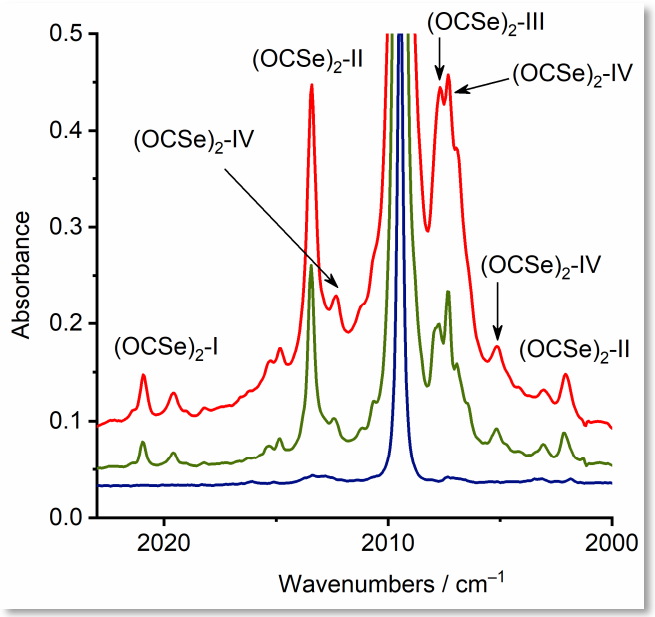

Figure 14. FTIR spectra in the ν(C=O) region of OCSe isolated in an Ar matrix at different OCSe:Ar ratios: 1:1000 (bottom, blue-trace), 1:500 (middle, green-trace), and 1:200 (top, red-trace). Bands assigned to four distinct dimeric species are indicated.

Self-aggregation in molecules capable of forming hydrogen bonds between a hydrogen atom of one unit and an oxygen atom of another unit can lead to stable cyclic structures. This is the case for the dimer of methyl thioglycolate ($CH_3OC(O)CH_2SH$), whose signals intensify as the matrix concentration increases [68]. Theoretically, the most stable dimer is stabilized by dual hydrogen-bonding, where the carbonyl O lone pairs interact with the σ*(S−H) orbitals. The simulated IR spectrum for this dimer agrees excellently with the experimental matrix-isolation spectrum. A similar cyclic structure was also found for the dichloroacetyl chloride dimer ($(ClC(O)CHCl_2)_2$) isolated in solid Ar [69].

More complex structures were found for homoaggregates (dimers and trimers) of CX_3Y molecules (X, Y = H, halogen). Several dimeric species were identified as corresponding to energy minima according to computational simulations for $(CH_3X)_2$ with X = Cl, Br, I [64,70] and also for $(CHBr_3)_2$ [71], with head-to-tail structures being the global minimum in each case and the one that best explains the spectral features attributed to the dimer in the FTIR spectra of the matrix-isolated species. Trimers were also detected for CH_3Br and $CHBr_3$, their signals becoming evident either with an increase in the proportion of the studied molecule in the matrix or upon annealing.

5. Elucidation of Photochemical Mechanisms in Matrix-Isolation Conditions

Another relevant application of matrix-isolation photochemistry is the elucidation of photochemical mechanisms. The cryogenic and isolation conditions enable the detection of reactive intermediates, free radicals, pre-reactive complexes, and other species, thereby facilitating mechanism determination. The strategy employed by our group involves recording IR spectra at different light exposure times, starting with very short intervals on the order of seconds and progressively increasing the duration throughout the experiment until a steady state is reached, marked by no further detectable changes in the spectra. Subsequent grouping of absorptions exhibiting identical kinetic behaviour is a primary step for identifying photoproducts. The effect of irradiation in different spectral regions on the mechanisms is also investigated.

As previously illustrated in this review with several examples, determining these mechanisms explains product formation and accounts for differences in systems that might initially be expected to behave similarly. For instance, the photochemical reaction between CO and Cl_2, BrCl, or ICl under matrix conditions yields the respective "phosgenes" (XC(O)Y), whereas, under the same experimental conditions, the equivalent $O{=}CBr_2$ is not formed [25]. This difference was attributed to the formation of a free $ClCO\cdot$ radical intermediate in the reactions with FCl, Cl_2, and ICl (see Scheme 5). In contrast, for bromine-containing analogues, no such radical was observed; instead, a weakly bound $CO\cdots Br$ complex was detected for the first time in this study, which does not lead to the formation of $O{=}CBr_2$. Another illustrative case involves the reactions between OCS and halogens or interhalogens, which lead to the formation of species with the general formula XC(O)SY, except for the reaction with Cl_2, where the main products are ClC(O)SSCl and the van der Waals complex $Cl_2C{=}O\cdots Cl_2$ [16]. This discrepancy is explained by the stoichiometry of the initial pre-reactive complexes. While 1:1 heteroaggregates form in the first case, the most stable species in the second are trimers.

The complex UV-vis photolysis of $CH_3C(O)SR$ molecules (R = H, CH_3, and $C(O)CH_3$) isolated in solid matrices proceeds through three alternative channels [48], as schematically represented in Scheme 7. The primary mechanism is the formation of ketene as a major product, together with the corresponding thiol RSH (where R = H, CH_3 and CH_3CO, respectively). A second channel involves CO extrusion and the formation of CH_3SX species, while a third pathway yields OCS and CH_3X. These latter two mechanisms coincide with those found for XC(O)SY species where X and Y are halogen atoms (as represented in Scheme 2). Some of the primary products are themselves photolabile. This is the case, for example, for $CH_3C(O)SH$ and $CH_3C(O)SCH_3$, which act as intermediates contributing to the unusually rich matrix photochemistry of diacetyl sulfide.

Similar mechanisms were observed for $CH_3C(O)SeH$ and its perdeuterated form, $CD_3C(O)SeD$, which also follow a three-channel photolysis mechanism with ketene as the major product [12]. A key difference is that CH_3SeH, formed in the second channel, is photolabile and decomposes presumably into $H_2C{=}Se$. Subsequently, the photochemistry of matrix-isolated diacetyl diselenide was also investigated. Interestingly, and in contrast to the previous systems, it proceeded via a single, clean pathway, producing ketene ($H_2C{=}C{=}O$), methylselane (CH_3SeH), and carbonyl selenide (OCSe) [58].

The presence of a perfluoroalkyl group alters the mechanism significantly. Thus, the photolysis of $CF_3C(O)SeH$ primarily yields CF_3SeH and CO, with HCF_3 and OCSe formed to a minor extent via a $CF_3\cdot$ radical-mediated pathway [13]. The differences in the main mechanism between $CH_3C(O)SeH$ and $CF_3C(O)SeH$ can be explained by considering that ketene formation is initiated by hydrogen atom detachment from a methyl group. This hypothesis is corroborated by two further examples: the photochemical mechanisms of $HCF_2C(O)SeH$ and $ClCF_2C(O)SeH$ [11]. For both acids, the main photochemical channel is the formation of the XCF_2SeH species (X = H, Cl) accompanied by CO extrusion. In an alternative channel, difluoroselenophosgene, $F_2C{=}Se$, is isolated. The nature of the third photochemical channel depends on the substituent X. When X is hydrogen, the third pathway yields difluoroketene, $F_2C{=}C{=}O$. However, when hydrogen is replaced by chlorine, difluoroketene is not formed. Instead, carbonyl selenide (OCSe), which forms molecular complexes with HCl, is produced, completing the array of photoproducts from $ClCF_2C(O)SH$.

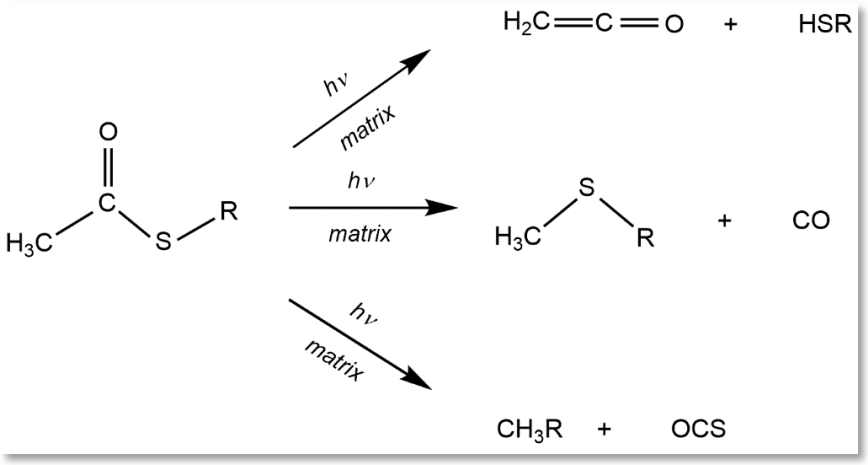

Scheme 7. Schematic representation of the three photoevolution mechanisms for matrix-isolated $CH_3C(O)SR$ molecules.

The formation of ketene molecules also dominated the photochemical behaviour of matrix-isolated thiolactones [72,73]. UV-vis irradiation of γ-butyrothiolactone in an argon matrix yields methylketene ($CH_3CH_2HC=C=O$) as the dominant product, contrasting with the gas-phase thermal reaction where decarbonylation is the principal mechanism. Similarly, β-propiothiolactone generates ketene ($CH_3HC=C=O$) under photolysis. This pattern indicates that the dominant photodecomposition channel for small thiolactones is sulfur atom elimination, forming the corresponding ketene. The prevalence of this channel suggests that photoevolution is driven by excited states localized on the -SC(O)- chromophore, a conclusion corroborated by He(I) photoelectron spectra confirming the significance of this group in the outermost valence electronic structure.

The versatility of the matrix-isolation approach in elucidating a wide array of photochemical pathways is further underscored by several key examples. In sulfur-rich systems, the photolysis of ClC(O)SSSC(O)Cl in argon and nitrogen matrices identified ClC(O)SSCl as a primary photoproduct, establishing a new pathway within this family of compounds [42]. Similarly, the irradiation of $(CH_3)_2CHOC(S)SC(O)OCH_3$, led to a complex mixture of products, including $CH_3OC(O)SCH(CH_3)_2$, OCS, CO, CO_2, and CS_2, while also providing scarce IR data for the $CH_3OC(O)SCH(CH_3)_2$ species [43]. A distinct dissociation channel was observed for $CF_3C(O)SC(CH_3)_3$ and $CF_3C(O)OC_5F_6$, where broad-band UV-vis irradiation primarily yielded $CF_3SC(CH_3)_3$ or $CF_3OC_5F_6$, respectively, and CO, offering direct insight into its gas-phase unimolecular reactivity under controlled conditions [74,75]. Moving to heterocumulene systems, the193 nm ArF excimer laser photolysis of $ClF_2CC(O)NCO$ in an argon matrix primarily produced ClF_2CNCO, with $ClF_2CC(O)N$ as a minor product [54], while the analogous photolysis of. $ClF_2CC(O)NCS$ yielded ClF_2CNCS, CO, and the rearrangement product $ClC(O)CF_2NCS$ [55].

In addition to the examples already presented, this technique is used by our group to study the mechanisms of photolysis and photochemical reactions of atmospheric interest. For example, methyl thioglycolate, $CH_3OC(O)CH_2SH$, was studied in matrix isolation conditions by FTIR spectroscopy, and the influence of molecular oxygen on its photochemical mechanisms was investigated [76]. The photoproducts detected without O_2 were CH_3OH, H_2CS, and CO, while SO_2, H_2CO, CH_4, and CO_2 were formed in the presence of molecular oxygen. These mechanisms contrast with those observed in the gas phase, where the products were $CH_3OC(O)CH_3$ and S_8 in the absence of O_2, and SO_2, CH_3OH, HC(O)OH, and CO in its presence. The primary difference between gas-phase and matrix conditions, apart from temperature, is the reaction molecularity. In contrast to the gas phase, matrix processes are predominantly unimolecular, with bimolecular reactions occurring to a lesser extent and depending on the relative proportions of the starting molecules and the stability of homo- or heteroaggregates.

Similarly, the photolysis mechanisms of dichloroacetyl chloride ($ClC(O)CHCl_2$), in the presence and absence of O_2, were determined [69]. This species is an intermediate in the photochemical reaction between trichloroethylene and oxygen, making it highly relevant to atmospheric chemistry. The matrix-isolation photochemical mechanisms were found to be wavelength-dependent. The compound was photostable when irradiated with light of wavelengths above 400 nm but yielded dichloroketene upon photolysis with light in the 280–320 nm and 350–450 nm spectral regions. Exposure of $ClC(O)CHCl_2$ to broad-band radiation (200–800 nm) produced dichloroketene as an intermediate photoproduct, followed by the formation of different 1:1 $CHCl_3$:CO molecular complexes after further irradiation. In the presence of oxygen, the photochemical mechanisms differed, producing $O=CCl_2$ and CO_2. In the gas phase, photolysis yielded HCl, CO, $CHCl_3$, and $ClC(O)CCl_2CCl_2H$, through a bimolecular mechanism involving insertion of the $:CCl_2$ biradical into a parent molecule's C–C bond. These mechanisms are summarised in Figure 15.

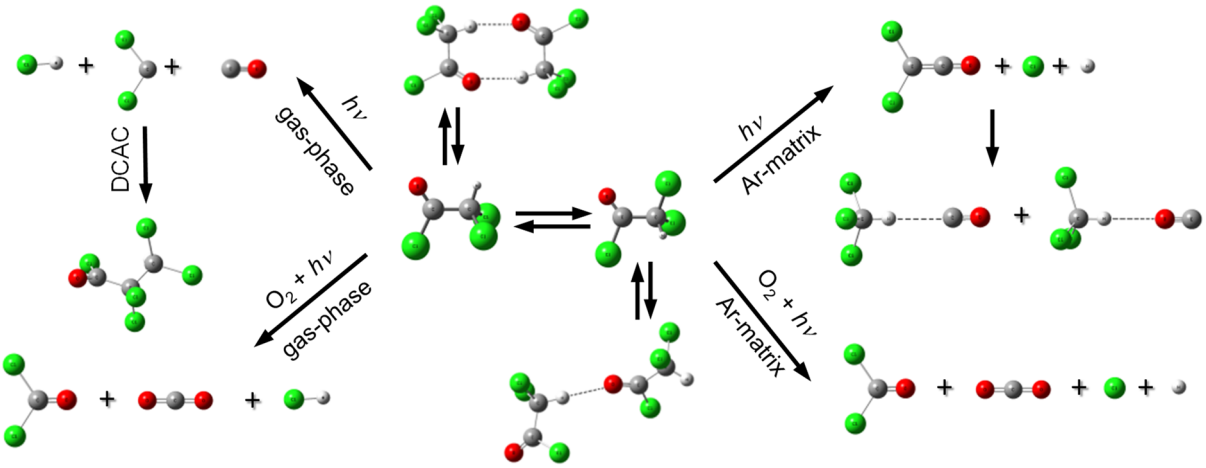

Figure 15. Outline of the photochemical mechanisms of dichloroacetyl chloride ($ClC(O)CHCl_2$, DCAC) isolated in Ar-matrix, in the presence and absence of O_2.

The photochemical behaviour of methyl iodide (CH_3I) on ice surfaces was investigated to assess its atmospheric implications [77]. The photochemical outcome was found to depend critically on the specific mode of interaction between CH_3I and the ice. A comparison between CH_3I adsorbed on ice and a CH_3I monomer complexed with water in cryogenic argon matrices revealed a key finding: CH_3I is resistant to photofragmentation when engaged in hydrogen bonding with the water/ice network, implying efficient energy dissipation into the hydrogen-bonded matrix. In contrast, the formation of a pnicogen-type I···O bond led to ready fragmentation, a result of intramolecular electronic relaxation. Therefore, water ice does not act as a catalyst for CH_3I photofragmentation but rather modifies the electronic relaxation pathways; dissociation occurs only through specific interaction modes. These results offer a molecular-level understanding of how water/ice–CH_3I interactions direct its atmospheric photochemical fate.

6. Matrix Isolation as a Characterization Tool

Matrix isolation at cryogenic temperatures remains as a standard method for characterizing molecular compounds, particularly species with sufficient vapour pressure to be diluted in an inert gas and deposited to achieve matrix conditions. The resulting vibrational spectrum provides critical information that can serve as the foundation for further studies or, in simpler cases, offer definitive characterization of novel species.

Our group routinely employs this technique, whenever feasible, as a primary characterization tool for novel compounds. A representative example is the characterization of $ClSO_2OOSO_2Cl$, a short-lived molecule (with a half-life of approximately 15 min) prepared by the photochemical reaction of $Cl_2/SO_2/O_2$ gas-phase mixtures at low temperature (−78 °C) [78]. The isolation and spectroscopic identification of this novel peroxide was a key achievement, with potential implications for understanding atmospheric processes on Venus. While DFT calculations indicated the presence of at least two rotamers at ambient temperature, matrix isolation in solid argon at 15 K enabled the exclusive characterization of the most stable conformer.

7. Conclusions

This review emphasised that matrix-isolation IR spectroscopy, particularly when synergistically combined with computational chemistry and photochemistry, constitutes a uniquely powerful methodology for advancing fundamental chemical knowledge. Its primary strength lies in its ability to stabilize and characterize novel molecules and elusive species, enabling their unambiguous generation and identification. Furthermore, the technique provides unparalleled detail in conformational analysis, allowing for the isolation and spectroscopic interrogation of individual conformers. It enables the detection of high-energy rotamers, whether they are present in the initial sample vapour and identified through the method's high sensitivity, or are generated in situ via photochemical processes within the matrix. It also offers a direct window into the formation and structures of molecular homo- and heteroaggregates through weak intermolecular forces. A critical application is the elucidation of intricate photochemical mechanisms by permitting the observation of reactive intermediates and pre-reactive complexes. Collectively, these capabilities provide profound, molecular-level insights into processes of atmospheric and astrochemical relevance, solidifying the role of matrix isolation as an indispensable tool in the modern chemical sciences.

Moving forward, the continued relevance of matrix-isolation studies will be driven by both methodological advances and the exploration of new scientific frontiers. Methodological progress is likely to focus on enhancing sensitivity, integrating complementary spectroscopic techniques, and refining theoretical models for more accurate predictions and spectral assignments. The method's unique capabilities ensure its expanding application in critical areas such as astrochemistry, for modelling molecular formation in interstellar environments, and atmospheric chemistry, for elucidating the interactions and photoprocesses of key reactive species. By continuing to bridge experiment and theory, matrix isolation will remain a fundamental tool for uncovering molecular-level mechanisms and driving discovery in both fundamental and applied chemical research.

Author Contributions

R.M.R. and C.O.D.V. contributed equally to the conceptualization, writing, and revision of this manuscript. All authors have read and agreed to the published version of the manuscript.

Funding

The authors acknowledge the Consejo Nacional de Investigaciones Científicas y Técnicas (CONICET) (PIP 0352 and PUE-2017-22920170100053), the Agencia Nacional de Promoción Científica y Tecnológica (ANPCyT) (PICT-2018-04355 and PICT-2020-03746), and the Universidad Nacional de La Plata (UNLP-X971) for providing financial support.

Institutional Review Board Statement

Not applicable.

Informed Consent Statement

Not applicable.

Data Availability Statement

The data that support the findings of this study are available from the corresponding author upon reasonable request.

Conflicts of Interest

The authors declare no conflict of interest.

Use of AI and AI-Assisted Technologies

No AI tools were utilized for this paper.

References

1. Whittle, E.; Dows, D.A.; Pimentel, G.C. Matrix Isolation Method for the Experimental Study of Unstable Species. *J. Chem. Phys.* **1954**, *22*, 1943–1943.
2. Fausto, R. *Low Temperature Molecular Spectroscopy*; NATO-ASI Series C483; Kluwer: Amsterdam, The Netherlands, 1996.
3. Varetti, E.L.; Pimentel, G.C. Isomeric forms of dinitrogen trioxide in a nitrogen matrix. *J. Chem. Phys.* **1971**, *55*, 3813–3821.
4. Willner, H. Das Infrarotspektrum von matrixisoliertem SFCl. *Z. Naturforsch. B* **1984**, *39*, 314–316.
5. Della Védova, C.O.; Mack, H.-G. A matrix photochemistry study on (fluorocarbonyl)sulfenyl bromide: The precursor of sulfur bromide fluoride. *Inorg. Chem.* **1993**, *32*, 948–950.
6. Romano, R.M.; Della Védova, C.O.; Downs, A.J.; et al. Matrix Photochemistry of *syn*-(Chlorocarbonyl)sulfenyl Bromide, *syn*-ClC(O)SBr: Precursor to the Novel Species *anti*-ClC(O)SBr, *syn*-BrC(O)SCl, and BrSCl. *J. Am. Chem. Soc*. **2001**, *123*, 5794–5801.
7. Romano, R.M.; Della Védova, C.O.; Downs, A.J. Matrix Photochemistry of the Chlorocarbonyl Sulfenyl Compounds ClC(O)SY, with Y = Cl or CH_3. *J. Phys. Chem. A* **2004**, *108*, 7179–7187.
8. Romano, R.M.; Della Védova, C.O.; Downs, A.J. Methanesulfenyl Fluoride, CH_3SF, a Missing Link in the Family of Sulfenyl Halides: Formation and Characterization through the Matrix Photochemistry of Methyl Thiofluoroformate, $FC(O)SCH_3$. *Chem. Eur. J.* **2007**, *13*, 8185–8192.

9. Rodríguez Pirani, L.S.; Erben, M.F.; Willner, H.; et al. $FC(O)SCH_2CH_3$: Spectroscopic and Computational Investigations. *J. Phys. Chem. A* **2014**, *118*, 11193–11203.
10. Gómez Castaño, J.A.; Romano, R.M.; Beckers, H.; et al. Preparation and Properties of Two Novel Selenoacetic Acids: $HCF_2C(O)SeH$ and $ClCF_2C(O)SeH$. *Inorg. Chem.* **2012**, *51*, 2608–2615.
11. Gómez Castaño, J.A.; Romano, R.M.; Beckers, H.; et al. Formation of the Matrix-Isolated Difluoromethylselanes XCF_2SeH (X = H, Cl) Through Photolysis of Selenoacetic Acids, $XCF_2C(O)SeH$. *Eur. J. Inorg. Chem.* **2013**, *2013*, 4585–4594.
12. Gómez Castaño, J.A.; Romano, R.M., Beckers, H.; et al. Selenoacetic Acid, $CH_3C(O)SeH$: Preparation, Characterization, and Conformational Properties. *Angew. Chem. Int. Ed.* **2008**, *47*, 10114–10118.
13. Gómez Castaño, J.A.; Romano, R.M., Beckers, H.; et al. Trifluoroselenoacetic acid, $CF_3C(O)SeH$: Preparation and Properties *Inorg. Chem.* **2010**, *49*, 9972–9977.
14. Juncal, L.C.; Cozzarín, M.V.; Romano, R.M. Conformational and spectroscopic study of xanthogen ethyl formates, $ROC(S)SC(O)OCH_2CH_3$. Isolation of $CH_3CH_2OC(O)SH$. *Spectrochim. Acta A* **2015**, *139*, 346–355.
15. Romano, R.M.; Della Védova, C.O.; Downs, A.J. (Bromocarbonyl) sulfenyl bromide, BrC(O)SBr: A novel carbonyl sulfenyl compound formed by the photochemical reaction between Br_2 and OCS isolated together in an Ar matrix. *Chem. Comm.* **2001**, 2638–2639. https://doi.org/10.1039/B108218C.
16. Tobón, Y.A.; Nieto, L.I.; Romano, R.M.; et al. Photochemical Reaction Channels of OCS with Cl_2, ICl, or IBr Isolated Together in an Argon Matrix: Isolation of syn-Iodocarbonylsulfenyl Bromide. *J. Phys. Chem. A* **2006**, *110*, 2674–2681.
17. Picone, A.; Della Védova, C.O.; Willner, H.; et al. Experimental and theoretical characterization of molecular complexes formed between OCS and XY molecules (X, Y = F, Cl and Br) and their role in photochemical matrix reactions. *Phys. Chem. Chem. Phys.* **2010**, *12*, 563–571.
18. Tobón, Y.A.; Romano, R.M.; Della Védova, C.O.; et al. Formation of New Halogenothiocarbonylsulfenyl Halides, XC(S)SY, Through Photochemical Matrix Reactions Starting from CS_2 and a Dihalogen Molecule XY (XY = Cl_2, Br_2 or BrCl). *Inorg. Chem.* **2007**, *46*, 4692–4703.
19. Custodio Castro, M.T.; Della Védova, C.O.; Willner, H.; et al. Ar-Matrix Studies of the Photochemical Reaction between CS_2 and ClF: Prereactive Complexes and Bond Isomerism of the Photoproducts. *Photochem* **2022**, *2*, 765–778.
20. Gómez Castaño, J.A.; Romano, R.M.; Willner, H.; et al. Preparation of the novel XC(O)SeX species (X = Cl, Br) through matrix photochemical reactions of OCSe with Cl_2 and Br_2 at cryogenic temperatures. *Inorg. Chim. Acta* **2008**, *361*, 540–550.
21. Gómez Castaño, J.A.; Romano, R.M.; Della Védova, C.O.; et al. Photochemical reaction of OCSe with ClF in argon matrix: A light-driven formation of XC(O)SeY (X, Y = F or Cl) species. *J. Phys. Chem. A* **2017**, 121, 2878–2887.
22. Cozzarín, M.V.; Romano, R.M.; Willner, H.; et al. Matrix isolation of the elusive fluorocarbonylsulfenyl fluoride molecule FC(O)SF. *J. Phys. Chem. A* **2013**, *117*, 855–862.
23. Gómez Castaño, J.A.; Picone, A.L.; Romano, R.M.; et al. Early Barriers in the Matrix Photochemical Formation of *syn–anti* Randomized FC(O)SeF from the $OCSe:F_2$ Complex. *Chem. Eur. J.* **2007**, *13*, 9355–9361.
24. Bava, Y.B.; Cozzarín, M.V.; Della Védova, C.O.; et al. Preparation of FC(S)SF, FC(S)SeF and FC(Se)SeF through matrix photochemical reactions of F_2 with CS_2, SCSe, and CSe_2. *Phys. Chem. Chem. Phys.* **2021**, *23*, 20892–20900.
25. Romano, R.M.; Della Védova, C.O.; Downs, A.J.; et al. New Members of an Old Family: Isolation of IC(O)Cl and IC(O)Br and Evidence for the Formation of Weakly Bound Br•···CO. *Inorg. Chem.* **2005**, *44*, 3241–3248.
26. Mack, H.-G.; Oberhammer, H.; Della Védova, C.O. Conformational properties and gas-phase structure of (fluorocarbonyl) sulfenyl chloride, FC(O)SCl; electron diffraction, vibrational analysis, and ab initio calculations. *J. Phys. Chem.* **1991**, *95*, 4238–4241.
27. Romano, R.M.; Della Védova, C.O.; Boese, R. Structural analysis, matrix Raman spectra, *syn–anti* photoisomerization and pre-resonance Raman effect of fluorocarbonylsulfenyl chloride, FC(O)SCl. *J. Mol. Struct.* **1999**, *513*, 101–108.
28. Romano, R.M.; Della Védova, C.O.; Downs, A.J.; et al. Structural and vibrational properties of ClC(O)SY compounds with Y = Cl and CH_3. *New J. Chem.* **2003**, *27*, 514–519.
29. Erben, M.F.; Della Védova, C.O.; Romano, R.M.; et al. Anomeric and Mesomeric Effects in Methoxycarbonylsulfenyl Chloride, $CH_3OC(O)SCl$: An Experimental and Theoretical Study. *Inorg. Chem*. **2002**, *41*, 1064–1071.
30. Spaltro, A.; Peluas, M.G.; Della Védova, C.O.; et al. Conformational Analysis of Trifluoroacetyl Triflate, $CF_3C(O)OSO_2CF_3$: Experimental Vibrational and DFT Investigation. *Spectrosc. J.* **2024**, *2*, 68–81.
31. Spaltro, A.; Leone, M.I.; Castillo Ortiz, D.F.; et al. Effect of UV-visible radiation on the conformational equilibrium of matrix-isolated 1,1,3–trichlorotrifluoroacetone. *J. Mol. Struct.* **2024**, *1327*, 141277.
32. Ramos, L.A.; Ulic, S.E.; Romano, R.M.; et al. Vibrational spectra, crystal structures, constitutional and rotational isomerism of FC(O)SCN and FC(O)NCS. *Inorg. Chem.* **2010**, *49*, 11142–11157.
33. Ramos, L.A.; Ulic, S.E.; Romano, R.M.; et al. Spectroscopic characterization and constitutional and rotational isomerism of ClC(O)SCN and ClC(O)NCS. *J. Phys. Chem. A* **2013**, *117*, 2383–2399.

34. Ramos, L.A.; Ulic, S.E.; Romano, R.M.; et al. Matrix Photochemical Study and Conformational Analysis of $CH_3C(O)NCS$ and $CF_3C(O)NCS$. *J. Phys. Chem. A* **2014**, *118*, 697–707.
35. Cozzarín, M.V.; Tong, S.; Ge, M.; et al. Preparation and Spectroscopic Studies of FC(O)SSCl. *Eur. J. Inorg. Chem.* **2016**, *36*, 5568–5574.
36. Cozzarín, M.V.; Romano, R.M. Unimolecular Photochemical Mechanisms of FC(O)SSCl Isolated in Solid Ar. *Chem. Select* **2017**, *2*, 4092–4098.
37. Tobón, Y.A.; Cozzarín, M.V.; Wang, W.-G.; et al. Vibrational and Valence Photoelectron Spectroscopies, Matrix Photochemistry and Conformational Studies of ClC(O)SSCl. *J. Phys. Chem. A* **2011**, *115*, 10203–10210.
38. Custodio Castro, M.T.; Della Védova, C.O.; Romano, R.M. Exploring Conformational Preferences in XC(W)ZY Molecules With X, Y = F, Cl, Br and W, Z = O, S, Se: Unraveling the Influence of Conjugative and Anomeric Interactions. *J. Phys. Org. Chem.* **2024**, *37*, e4654.
39. Della Védova, C.O.; Downs, A.J.; Novikov, V.P.; et al. Fluorocarbonyl Trifluoromethanesulfonate, $FC(O)OSO_2CF_3$: Structure and Conformational Properties in the Gaseous and Condensed Phases. *Inorg. Chem.* **2004**, *43*, 4064–4071.
40. Della Védova, C.O.; Downs, A.J.; Moschioni, E.; et al. Chlorocarbonyl Trifluoromethanesulfonate, $ClC(O)OSO_2CF_3$: Structure and Conformational Properties in the Gaseous and Condensed Phases. *Inorg. Chem.* **2004**, *43*, 8143–8149.
41. Trautner, F.; Della Védova, C.O.; Romano, R.M.; et al. Gas Phase structure and conformational properties of chlorocarbonyl trifluoromethanesulfonate, $ClC(O)OSO_2CF_3$. *J. Mol. Struct.* **2006**, *784*, 272–275.
42. Tobón, Y.A.; Cozzarín, M.V.; Della Védova, C.O.; et al. Experimental and Theoretical Studies on Bis(Chlorocarbonyl)trisulfane, ClC(O)SSSC(O)Cl. *J. Mol. Struct.* **2009**, *930*, 37–42.
43. Tobón, Y.A.; Romano, R.M.; Hey-Hawkins, E.; et al. A comprehensive study of $(CH_3)_2CHOC(S)SC(O)OCH_3$ using matrix isolation technique, X-ray analysis, spectroscopic studies and theoretical calculations. *J. Phys. Org. Chem.* **2009**, *22*, 815–822.
44. Berrueta Martínez, Y.; Reuter, C.G.; Vishnevskiy, Y.V.; et al. Structural Analysis of Perfluoropropanoyl Fluoride in the Gas, Liquid and Solid Phases. *J. Phys. Chem. A*, **2015**, *120*, 2420–2430.
45. Arce, V.B.; Czarnowski, J.; Romano, R.M. Bromodifluoroacetyl fluoride, $CF_2BrC(O)F$: Experimental and theoretical studies. *J. Mol. Struct.* **2006**, *825*, 32–37.
46. Arce, V.B.; Della Védova, C.O.; Downs, A.J.; et al. Trichloromethyl Chloroformate ("Diphosgene"), $ClC(O)OCCl_3$: Structure and Conformational Properties in the Gaseous and Condensed Phases. *J. Org. Chem.* **2006**, *71*, 3423–3428.
47. Della Védova, C.O.; Romano, R.M.; Stammler, H.-G.; et al; Perfluoropropionic Acid ($CF_3CF_2C(O)OH$): Three Conformations and Dimer Formation. *Molecules* **2025**, *30*, 1887.
48. Romano, R.M.; Della Védova, C.O.; Downs, A. Matrix photochemistry of $CH_3C(O)SX$ molecules with X = H, CH_3, and $C(O)CH_3$: Formation of ketene in another decomposition channel of sulfenyl carbonyl compounds. *J. Phys. Chem. A* **2002**, *106*, 7235–7244.
49. Arango Hoyos, B.E.; Romano, R.M. Experimental and theoretical conformational studies on diallyl sulfide. *J. Mol. Struct.* **2019**, *1182*, 54–62.
50. Ramos, L.A.; Ulic, S.E.; Romano, R.M.; et al. Chlorodifluoroacetyl Cyanide, $ClF_2CC(O)CN$: Synthesis, Structure, and Spectroscopic Characterization. *Inorg. Chem.* **2011**, *50*, 9650–9659.
51. Tobon, Y.A.; Di Loreto, H.E.; Della Védova, C.O.; et al. Matrix isolation study of ethyl chloroformate, $ClC(O)OCH_2CH_3$. *J. Mol. Struct.* **2008**, *881*, 139–145.
52. Moreno Betancourt, A.; Schwabedissen, J.; Romano, R.M.; et al. Disulfuryl dichloride $S_2O_5Cl_2$—A conformational and polymorphism chameleon. *Chem. Eur. J.* **2018**, *24*, 10409–10421.
53. Romano, R.M.; Moreno Betancourt, A.; Della Védova, C.O.; et al. Preparation and properties of chlorosulfuryl chloroformiate, $ClC(O)OSO_2Cl$. *Inorg. Chem.* **2018**, *57*, 14834–14842.
54. Ramos, L.A.; Ulic, S.E.; Romano, R.M.; et al. Chlorodifluoroacetyl isocyanate, $ClF_2CC(O)NCO$: Preparation and structural and spectroscopic studies. *J. Phys. Chem. A* **2012**, *116*, 11586–11595.
55. Ramos, L.A.; Ulic, S.E.; Romano, R.M.; et al. Chlorodifluoroacetyl Isothiocyanate, $ClF_2CC(O)NCS$: Preparation and Structural and Spectroscopic Studies. *J. Phys. Chem. A* **2013**, *117*, 5597–5606.
56. Cánneva, A.; Erben, M.F.; Romano, R.M.; et al. The Structure and Conformation of $(CH_3)_3CSNO$. *Chem. Eur. J.* **2015**, 21, 10436–10442.
57. Ramos, L.A.; Ulic, S.E.; Romano, R.M.; et al. Dimers of Perhaloacetyl Cyanides: $CClF_2C(O)OC(CN)_2CClF_2$ and $CF_3C(O)OC(CN)_2CF_3$. Preparation, Properties, and Spectroscopy. *J. Phys. Chem. A* **2014**, *118*, 1721–1729.
58. Gómez Castaño, J.A.; Romano, R.M.; Salamanca, A.R.; et al. Vibrational spectra, conformational properties and argon matrix photochemistry of diacetyl diselenide, $CH_3C(O)Se_2C(O)CH_3$. *J. Phys. Org. Chem.* **2016**, *29*, 636–644.
59. Robles, N.L.; Antognini, A.F.; Romano, R.M. Formation of XNCO Species (X = F, Cl) through Matrix-Isolation Photochemistry of XSO_2NCO Molecules. *J. Photochem. Photobiol. A* **2011**, *223*, 194–201.

60. Romano, R.M.; Downs, A.J. Matrix-Isolated Van der Waals Complexes Formed between CO and Dihalogen Molecules XY with X, Y = Cl, Br, or I. *J. Phys. Chem. A* **2003**, *107*, 5298–5305.
61. Romano, R.; Picone, A.; Downs, A.J. Matrix-Isolated van der Waals Complexes Formed between CS_2 and Dihalogen Molecules XY, Where XY = Cl_2, Br_2, BrCl, ICl, or IBr. *J. Phys. Chem. A* **2006**, *110*, 12129–12135.
62. Picone, A.; Romano, R.M. Infrared matrix-isolation studies of the $CS_2\cdots HCl$ molecular complex. *J. Mol. Struct.* **2010**, *978*, 187–190.
63. Gómez Castaño, J.A.; Fantoni, A.; Romano, R.M. Matrix isolation FTIR study of carbon dioxide: Reinvestigation of the CO_2 dimer and $CO_2\cdots N_2$ complex. *J. Mol. Struct.* **2008**, *881*, 68–75.
64. Custodio-Castro, M.T.; Coussan, S.; Mascetti, J.; et al. Molecular-Level Insights of Interaction between Bromomethane and Water: Infrared Matrix-Isolation and Theoretical Studies. *J. Phys. Chem. A* **2025**, *129*, 6082–6093.
65. Spaltro, A.; Leone, M.I.; Della Védova, C.O.; et al. A New Step in Understanding the Process of Lithium Battery Manufacturing Process. Analysis of the $CH_3CN–PF_5$ Species in Matrices at Cryogenic Temperatures. *Phys. Chem. Chem. Phys.* **2026**, *28*, 1420–1428.
66. Leone, M.I.; Custodio Castro, M.T.; Spaltro, A.; et al. CEQUINOR, La Plata, Argentina. 2026, *manuscript in preparation.*
67. Gómez-Castaño, J.A.; Romano, R.M. Matrix isolation studies of carbonyl selenide, OCSe: Evidence of the formation of dimeric species, $(OCSe)_2$. *J. Vib. Spectrosc.* **2013**, *70*, 28–35.
68. Bava, Y.B.; Tamone, L.M.; Juncal, L.C.; et al. Experimental and theoretical IR study of methyl thioglycolate, $CH_3OC(O)CH_2SH$, in different phases: Evidence of a dimer formation. *J. Mol. Struct.* **2017**, *1139*, 160–165.
69. Tamone, L.M.; Picone, A.L.; Romano, R.M. New insights into the Ar-matrix-isolation FTIR spectroscopy and photochemistry of dichloroacetyl chloride, $ClC(O)CHCl_2$: Influence of O_2 and comparison with gas-phase photochemistry. *J. Photochem. Photobiol.* **2021**, *6*, 100019.
70. Sobanska, S.; Houjeij, H.; Coussan, S.; et al. Infrared matrix-isolation and theoretical studies of interactions between CH_3I and water. *J. Mol. Struct.* **2021**, *1236*, 130342.
71. Custodio Castro, M.T.; Leone, M.I.; Tamone, L.M.; et al. CEQUINOR, La Plata, Argentina. 2026, *manuscript in preparation.*
72. Dugarte, N.Y.; Erben, M.F.; Romano, R.M.; et al. Matrix Photochemistry at Low Temperatures and Spectroscopic Properties of γ-Butyrothiolactone. *J. Phys. Chem. A* **2010**, *114*, 9462–9470.
73. Dugarte, N.Y.; Erben, M.F.; Romano, R.M.; et al. Matrix Photochemistry, Photoelectron Spectroscopy, Solid-Phase Structure, and Ring Strain Energy of β-Propiothiolactone. *J. Phys. Chem. A* **2009**, *113*, 3662–3672.
74. Cayón, V.M.; Erben, M.F.; Romano, R.M.; et al. Structure, Conformational Properties and Matrix Photochemistry of S-(tert-butyl)trifluorothioacetate $CF_3C(O)SC(CH_3)_3$. *New J. Chem.* **2020**, *44*, 14568–14577.
75. Cayón, V.M.; Erben, M.F.; Romano, R.M.; et al. Spectroscopic and Structural Studies on Phenyl and Pentafluorophenyl Trifluorothioacetate, and Pentafluorophenyl Trifluoroacetate, $CF_3C(O)SC_6H_5$, $CF_3C(O)SC_6F_5$ and $CF_3C(O)OC_6F_5$. *Phys. Chem. Chem. Phys.* **2023**, *25*, 9394–9403.
76. Bava, Y.B.; Tamone, L.M.; Juncal, L.C.; et al. Gas-phase and matrix-isolation photochemistry of methyl thioglycolate, $CH_3OC(O)CH_2SH$: Influence of the presence of molecular oxygen in the photochemical mechanisms. *J. Photochem. Photobiolog. A* **2017**, *344*, 101–107.
77. Custodio-Castro, M.T.; Romano, R.M.; Mascetti, J.; et al. Photochemistry of $CH_3I\cdots(H_2O)n$ Complexes: From $CH_3I\cdots H_2O$ to CH_3I in Interaction with Water Ices and Atmospheric Implication. *ACS Earth Space Chem.* **2024**, *8*, 992–999.
78. Romano, R.M.; Della Védova, C.O.; Beckers, H.; et al. Photochemistry of $SO_2/Cl_2/O_2$ Gas Mixtures: Synthesis of the New Peroxide $ClSO_2OOSO_2Cl$. *Inorg. Chem.* **2009**, *48*, 1906–1910.